2013

Thompson-Like Groups for Quadratic Rational Julia Sets

Jasper O. Weinrich-Burd
Bard College

A Thompson-Like Group for the Bubble Bath Julia Set

A Senior Project submitted to
The Division of Science, Mathematics, and Computing
of
Bard College

by
Jasper Weinrich-Burd

Annandale-on-Hudson, New York
May, 2013

Abstract

Julia sets are fractals that arise in the study of dynamical systems on the complex plane. Recently, Belk and Forrest investigated a group of "piecewise-linear" homeomorphisms on the Julia set for the function $f(z) = z^2 - 1$. This group closely resembles Thompson's group T, a finitely generated group of piecewise-linear functions on the unit circle. Inspired by Belk and Forrest's work, we examine the Julia set for the function $\phi(z) = z^{-2} - 1$, which we refer to as the Bubble Bath. Because ϕ is rational, the external angles used by Belk and Forrest are not available. Instead our approach makes heavy use of symbolic dynamics. In particular, we show how to assign an address to every point in the Bubble Bath. We use these addresses to define a group T_{BB}. We prove that T_{BB} is generated by four elements, that it contains T, and that it is a semi-direct product of its double commutator subgroup with S_3. We also prove that its double commutator subgroup is an infinite simple group. Finally, we briefly investigate homeomorphisms of certain other rational Julia sets.

Contents

List of Figures

Dedication

Dedicated to Claire Martin, who sees me how I want to be. I look forward to exploring a new world with you next year. I look forward to our next life together.

Acknowledgments

Jim Belk has been the best project advisor I could have ever imagined. His enthusiasm, encouragement, commitment, clarity, and contagious curiosity are an inspiration. I must also thank Maria, for so generously lending him out.

I want to acknowledge the rest Math Program for four years of support. In particular, thanks to John for advising me in a big way. Thanks for innumerable eye-opening classes and conversations. Thanks to Greg for introducing me to higher mathematics by teaching my first proofs course and supervising my first mathematics research. Thanks to Lauren for her help in considering graduate school options and always caring about what's happening in our lives. Lastly, thanks to Loek Helminck, Ruth Haas, and Emma Norbrothen for giving me my first taste of non-Bard mathematics. Thanks to my many classmate, particularly Emily, Fanny, Matt, Will, and Ian.

Thanks to my friends for their continued affection, even when I thought I was too busy to spend time with them. Thanks to my team, you have taught me so much about myself. Special thanks to Steve.

Finally, thank you Mom and Dad.

Introduction

This project is about an interesting overlap between dynamical systems and group theory. Dynamical systems is the study of systems that change over time. It is often used in applied mathematics to model heat or fluid flow, financial fluctuation, or movement and randomness in computer graphics. Although it is known for this relationship with the idea of *chaos*, it is also known for giving rise to self-symmetric objects called fractals. In particular, we study fractal-like sets called Julia sets which come from iterating holomorphic functions on the complex planeor Riemann sphere.

The study of complex dynamics began as early as the late nineteenth century. Pierre Fatou and Gaston Julia, names which the reader will recognize later in definitions and theorems, worked somewhat later – around 1920. Much of their work, however, did not come to prominence until Benoit Mandelbrot popularized and expanded it with the aid of computer visualization in the 1970's and 80's. In particular, the fractal set called the Mandelbrot set has become a famous image and an icon for the idea of a fractal. The Mandelbrot set visually and geometrically describes a classification of Julia sets of quadratic polynomial functions. The Julia sets we explore here are also fractal in nature but are

intrinsically different than the ones appearing in the Mandelbrot set because they come from rational functions. We mostly turn to [13] for the theory of these holomorphic rational functions.

We study the geometric symmetries of a Julia set by constructing a group of these symmetries and examining its properties. Because of their fractal nature, Julia sets are equally "rough" no matter how much you zoom in on their edges. This "roughness" comes from the fact that a Julia set is made up of small parts, which are each similar to the whole and made up of smaller parts, which are each similar to the whole, and so on. It is easy to see how such a set would be rich in symmetries. The group that we construct belongs to a unique and interesting type of group first discovered by Richard Thompson.

In 1965, Richard Thompson constructed the groups F, T, and V. These are groups of piecewise-linear homeomorphisms of the unit interval, the unit circle, and the Cantor set respectively. These groups have interested geometric group theorists for their unique combination of properties. For instance, Higman shows in [11] that T and V are examples of infinite simple groups with a finite presentation. They were among the first such groups. Furthermore, many standard geometric group theory techniques fail when applied to F, T, or V. There are basic geometric questions about these groups that have remained open for over forty years e.g. the amenability of F. Additionally, they seem to arise in a variety of areas of mathematics. This has led to numerous attempts to generalize them. For exposition on some of these and other results see [9], [5], and [6]. One recent generalization is that found in [4], which examines a group of homeomorphisms of a Julia set – quite a bit more complicated than the unit interval.

The basis for this project is the work in [4] by Belk and Forrest. They construct a Thompson-like group T_B on a Julia set called the Basilica that comes from a quadratic polynomial function $\phi(z) = z^2 - 1$. They assign "external angles" to points on the border of the Basilica. They use these angles to prove all of their subsequent results. They prove

that T_B contains an isomorphic copy of Thompson's group T, that T_B is generated by four elements, and that the commutator subgroup $[T_B, T_B]$ is simple and has index two.

We have a number of similar results for our group, however, we came to them in a different and more general way. The difference stems from the fact that our function $\phi(z) = \frac{1-z^2}{z^2}$ is rational – rather than polynomial. One consequence of this is that the structure of our Julia set is so fundamentally dissimilar from that of the Basilica that we cannot use the external angles which gave Belk and Forrest a way to refer to the points of the Basilica. Instead, we use a Markov partition to develop a system of addresses based in the dynamics of ϕ. The entirety of Chapter 2 is devoted to constructing these addresses. This method is very effective and is likely to generalize to an entire class of rational functions called hyperbolic. For this reason, it is perhaps the most important piece of the project, even though it is not included among the main results in Chapter 3.

Once we have this address system, it allows us to define our group T_{BB}. At this point we use some of the same techniques as Belk and Forrest. We produce a generating set with four elements. We show that there is an isomorphic copy of Thompson's group T in T_{BB}. We show that there is an index-six subgroup $K \leq T_B B$ and that it is generated by six copies of T. We prove that K is simple and further that all normal subgroups of $T_B B$ must contain K. Finally, we show that K is the double commutator subgroup. There are some differences between our results and those in [4]. In particular, our group seemed so similar that it was surprising when we discovered a non-abelian quotient and that $[T_{BB}, T_{BB}]$ was not simple

The remainder of the paper is organized as follows.

Chapter 1 encompasses basic background in a number of subjects. We use [1] for the basic definitions from dynamical systems and symbolic dynamics. We define Julia sets and give some theorems about holomorphic dynamics with the help of [13]. We use [9] to

introduce Thompson's Group T. Finally we discuss the methods and results of [4] which served as the main motivation for this work.

Chapter 2 introduces the Julia set for our function $\phi(z) = \frac{1-z^2}{z^2}$. We call this Julia set the Bubble Bath, see Figure 1.4.3, because of its many "bubbles". We difficulties that arise from using a rational function – rather than a polynomial as in [4]. Then we develop a geometric address system for labeling points of the Bubble Bath. This allows us to proceed with defining our group T_{BB}.

In Chapter 3 we define our group T_{BB} of "orientation preserving piecewise-linear homeomorphisms" on the geometric addresses Ω_{geom} and prove our main results mentioned above. These results are similar to those proved by Belk and Forrest in [4]. However, this only underlines the fact that using the geometric address system is a new and powerful method. We expect that this method of linking the dynamics of a function to its geometry should work well for many rational functions. Our technique should extend Belk and Forrest's work from the polynomial case, not just from the Basilica case.

In the last chapter, we present some preliminary exploration of a few other rational Julia sets and discuss directions for future work.

1
Preliminaries and Background

In this chapter we will provide the necessary background in dynamical systems, in the subfield of symbolic dynamics, in Julia sets, in Thompson's Group T, and finally in the paper [4] which served as the main motivation for this work. We assume a basic knowledge of real analysis, abstract algebra, and some topology.

In Section 1.1 we introduce the basic definition of a dynamical system, a state space, orbits, fixed points and cycles, and attracting points and cycles. These come mostly from [1]. We give a long example (also from [1]) in Section 1.2 in order to develop the reader's intuition about the concept of itineraries. The set of itineraries is an address system for points in a Julia set which we use as the basis for the symbolic dynamics approach in Section 2.1. We give rigorous definitions from [13] and [12] of Markov partition, transition graph, symbol space, itinerary, and Mealy machine in Section 1.3. In Section 1.4, we again use [13] to develop the definition of Julia set for our rational function $\phi(z) = \frac{1-z^2}{z^2}$. Then, Section 1.5 includes a brief introduction to Thompson's group T and draws from [9] and [4]. In the final section of background, we describe the method of external angles employed in [4] and their main results. Particularly, they proved that their group T_B contains a

copy of Thompson's group T, that it is finitely generated by four elements, and that the commutator subgroup $[T_B, T_B]$ is simple and has index two.

1.1 Dynamical Systems

A dynamical system can be a tricky thing to define. Weather is a famous dynamical system. There are rules of gravity, air pressure, and heat transfer that produce a wide range of conditions - everything from calm skies and glassy water to roiling seas and stormy nights. Weather is the classic example of the "butterfly effect" which states that a small deviation at the beginning, can have massive effects later on without introducing any element of randomness. Quite generally, a dynamical system is a

- set of deterministic rules acting to produce
- chaotic behavior.

The weather is not decided by random changes in the rules, it is simply very hard to predict what these rules will produce very far in the future. The butterfly effect beautify illustrates what we mean when we say *chaos*. However, to come to a more mathematical definition of a dynamical system, we will have to choose a simpler example.

Consider an accelerating runner who, after every second, is twice as far from the starting line as she was one second ago. If the runner is 2 meter from the starting line 0 second into the race, then she will be 4 meters away at 1 seconds, 8 meters at 2, and so on until she is $32,768$ meters away after just 14 seconds. However, if the runner is 2.1 meters from the starting line at 1 second, then at 14 seconds she will be $68,122.3$ meters into the race. Her progress is more than double what it was before! The runner's position is chaotic in the sense that a change of only 0.1 meters at the beginning produced a huge change is the later position, certainly enough to make the difference between a 3^{rd} and 1^{st} place finish.

Now that we've developed some intuition, we will make this idea more rigorous.

Definition 1.1.1. A **dynamical system** is an ordered pair (X, ϕ) where X is a topological space called the **state space** and ϕ is a function or **map** $\phi\colon X \to X$. △

Definition 1.1.2. The **orbit** of a point $x_0 \in X$ is the set $\{x_0, \phi(x_0), \phi(\phi(x_0)), f^{\circ 3}(x_0), \dots\}$ of repeated iterations of ϕ on x_0. The starting point x_0 of an orbit is called the **initial value**. The nth iteration applied to the initial value is often referred to as x_n so that an orbit might be written $\{x_0, x_1, x_2, \dots\}$. △

In our narrative above, the state space was the set of all possible distances from the starting line $\mathbb{R}_{>0}$. The map was $\phi(x) = 2x$. We examined the orbits of ϕ with initial value $x_0 = 2$ and $x_0 = 2.1$. We can compute more complete orbits:

$$\text{orbit of } 2 = \{2, 4, 8, 16, 32, 64, 128, 256, 512, 1024, 2048, 4096, 8192, 16384, 32768, \dots\}$$

$$\text{orbit of } 2.1 = \{2.1, 4.4, 9.2, 19.4, 40.8, 85.7, 180.1, 378.2, 794.2,$$

$$1667.9, 3502.7, 7355.8, 15447.2, 32439.2, 68122.3, \dots\}$$

Now we can see that there are big differences in these orbits even by the fifth or sixth iterations. To rigorously say that we are encountering a "butterfly effect", henceforth called **sensitive dependence on initial conditions**, we must examine the limits of these orbits as sequences. It's clear that the limit of each of these orbits diverges, but we can also see that one is diverging much faster. In particular, the limit of the difference of the two orbits diverges and thus ϕ exhibits sensitive dependence on initial conditions - chaos. We can also find orbits that don't diverge.

For the function ϕ above, the only orbit that doesn't diverge is the orbit of 0, which is just an infinite sequence of 0's. In this case we see that $\phi(0) = 0$. More generally, we call any x_0 such that $\phi(x_0) = x_0$ a **fixed point** of ϕ. To introduce further concepts we will need a more interesting example.

Example 1.1.3. Let $f\colon S^1 \to S^1$ where $S^1 \in \mathbb{C}$ is the unit circle in the complex plane and f doubles angles so that $f(e^{\theta i}) = e^{2\theta i}$. Consider the following orbits

$$\begin{aligned}
\text{orbit of } e^{\pi i/3} &= \{e^{i\pi/3}, e^{2i\pi/3}, e^{4i\pi/3}, e^{8i\pi/3}, e^{16i\pi/3}, e^{32i\pi/3}, e^{64i\ \pi/3}, e^{128i\pi/3}, \dots\} \\
&= \{e^{i\pi/3}, e^{2i\pi/3}, e^{i\pi/3}, e^{2i\pi/3}, e^{i\pi/3}, e^{2i\pi/3}, e^{i\pi/3}, e^{2i\pi/3}, \dots\} \\
\text{orbit of } e^{\pi i/15} &= \{e^{i\pi/15}, e^{2i\pi/15}, e^{4i\pi/15}, e^{8i\pi/15}, e^{16i\pi/15}, e^{32i\pi/15}, e^{64i\pi/15}, e^{128i\pi/15}, \dots\} \\
&= \{e^{i\pi/15}, e^{2i\pi/15}, e^{4i\pi/15}, e^{8i\pi/15}, e^{1i\pi/15}, e^{2i\pi/15}, e^{4i\pi/15}, e^{8i\pi/15}, \dots\}
\end{aligned}$$

In the first orbit, we just see the same two points repeated. In the second one we have a sequence of four points repeating themselves. ◊

Definition 1.1.4. A **periodic point** of a function f with **period** k is any point p such that $f^k(p) = p$. The orbit of such a point $\{p, f(p), f^2(p), \dots, f^k(p)\}$ is called a k-**cycle**. △

In the next example, we have an orbit that **converges** to a 2-cycle. When we say this what we mean is that the difference of the orbit and the 2-cycle converges to zero.

Example 1.1.5. Let $f(x) = 1 - x^2$. We note that the points 0 and 1 form a 2-cycle. Since $f(-0.5) = 0$, the orbit of -1 is *mostly* just this 2-cycle because -1 *leads in* to it after 1 iteration. There are other initial values whose orbits converge to the 2-cycle. Sometimes they hit it exactly as -1 does, and some times they approach it at infinity. Consider the three orbits graphed in Figure 1.1.1. The red is the orbit of -0.5, the blue is the orbit of 1.5, and the green is the orbit of 1.64. The red and blue are clearly both converging to the 2-cycle while the green diverges to infinity. So there is a set of points have converge to the 2-cycle and some other points don't. ◊

Definition 1.1.6. A fixed point p of a function f is **attracting** if the orbits of initial values in a neighborhood of p converge to p. A fixed point p is called **repelling** if there is a neighborhood of p such that no initial value in the neighborhood yields an orbit that converges to p. These definitions extend naturally to cycles. △

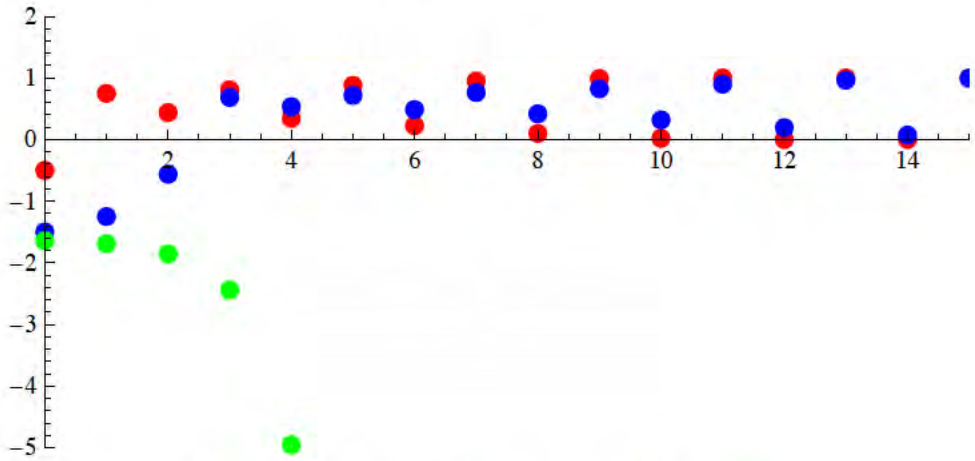

Figure 1.1.1: Orbits of -0.5, -1.5, and -1.64.

The following theorem tells us how to determine whether a cycle (or fixed point) is attracting or repelling.

Theorem 1.1.7 (Stability Test). *Let $c = \{p_1, p_2, \ldots, p_k\}$ be a k-cycle under ϕ. If*

$$|\phi'(p_1)\phi'(p_2)\ldots\phi'(p_k)| < 1,$$

then the periodic orbit of c is attracting. If

$$|\phi'(p_1)\phi'(p_2)\ldots\phi'(p_k)| > 1,$$

then the periodic orbit of c is repelling.

Definition 1.1.8. The **basin of attraction** of an attracting cycle C is an open set U that consists of all points $p \in X$ for which successive iterates $\phi^{\circ k}(p), \phi^{\circ 2k}(p)\ldots$ converge to some point in C. △

1.2 Tent Map

In order to analyze our complicated Julia sets it is necessary to develop some symbolic tools. In this section, we explore the ideas that we'll need through an in depth example. For rigorous definitions and theorems, the reader should look ahead to Section 1.3.

Figure 1.2.1: The Tent Map with a labeled subdivision of the domain.

The main idea is that of an **itinerary**. Given some dynamical system, every point in the state space can be assigned an itinerary. An itinerary is a kind of address for the point based on the dynamics of ϕ on the state space. An itinerary is an infinite sequence of symbols, herein capital roman letters.

Example 1.2.1 (Tent Map)**.** Let $\phi\colon [0,1] \to [0,1]$ be a function defined by

$$\phi(x) = \begin{cases} 2x & \text{if } 0 \leq x \leq \frac{1}{2} \\ 2 - 2x & \text{if } \frac{1}{2} \leq x \leq 1 \end{cases}$$

See Figure 1.2.1 for a graph of ϕ $\Diamond$

Definition 1.2.2. Let the symbols $\mathsf{L} = [0, \frac{1}{2}]$ and $\mathsf{R} = [\frac{1}{2}, 1]$. From here on, we use the words symbol and interval interchangeably to mean these objects.

Let $p \in [0,1]$ and let $\{S_k\}_{k=0}^{\infty}$ be a sequence with each $S_k \in \{\mathsf{L}, \mathsf{R}\}$. The sequence $\{S_k\}_{k=0}^{\infty}$ is an itinerary for p if $\phi^{\circ k}(p) \in S_k$ for all k. $\triangle$

Claim 1.2.3. *Given a point $p \in [0,1]$, we can compute an itinerary for p.*

Example 1.2.4. Consider the point 0.14 with (partial) orbit

$$\{0.14, 0.28, 0.56, 0.88, 0.24, 0.48, 0.96, 0.08, 0.16, 0.32\}.$$

Since $0.14 \in [0, \frac{1}{2}]$, the itinerary begins with an L. Then 0.28 gives us another L, but then we have $0.56 \in$ R and $0.88 \in$ R. Thus, the first ten letters in the itinerary are

LLRRLLRLLL. ◊

We could continue this indefinitely to determine the full itinerary from a full orbit. But note that for other points, this procedure could lead to multiple itineraries. Take for example, the point $\frac{1}{4}$ whose itinerary begins with L, but then can be followed by an L or an R because $\frac{1}{2}$ is in both. This is really just fine though, because more often we use itineraries to find points. In fact, given an itinerary, we can find a unique point. However this is slightly more complicated, so first we will need a lemma.

Claim 1.2.5. *Let S be the set of points whose itinerary begin with a finite sequence. Then S is a closed interval.*

Example 1.2.6. Consider the finite itinerary

LLR.

Clearly S is infinite, because we could have any number of endings after this simple beginning. The orbits of the points in S all begin in L, stay in L for one iteration, and then go to R. So from the first L we conclude that $S \subseteq [0, \frac{1}{2}]$. From the second L we conclude that $S \subseteq [0, \frac{1}{4}]$. The R tells us that $S \subseteq [\frac{1}{8}, \frac{1}{4}]$. If we think about it, we can confirm that the last containment is in fact an equality. ◊

This argument will work for any finite itinerary, so we can label subintervals of $[0, 1]$ with finite itineraries.

Beginning with our two intervals L and R, the rules for labeling subintervals are determined by ϕ. Here the following rule will produce the intervals in Figure 1.2.2.

Figure 1.2.2: Collections of 2^n subintervals of $[0,1]$ for $n \leq 3$.

- Suppose we have an interval with finite itinerary μ. It splits in half into two subintervals. The one on the left has itinerary $\mu\mathsf{L}$, the one on the right has itinerary $\mu\mathsf{R}$. Switch the order if there an odd number of R's in μ.

Suppose we consider the collection of all finite itineraries with n symbols. Then this rule leads to a collection of 2^n subintervals of $[0,1]$ which only overlap at their endpoints.

Proposition 1.2.7. *Given some sequence $\{S_k\}_{k=0}^{\infty}$ in $\{\mathsf{L},\mathsf{R}\}^{\infty}$, there is a unique point p such that $\{S_k\}_{k=0}^{\infty}$ is an itinerary for p.*

Proof. Consider any infinite symbol sequence I. Take the sequence of finite symbol subsequences of I in order of length. This gives us a sequence of nested closed intervals. Each interval is half as long as the one previous. Thus the lengths of the intervals goes to zero. By the Nested Interval Theorem, the intersection of our sequence of nested closed intervals with length going to zero is a single point p. This point p has I as its itinerary. □

Example 1.2.8. Consider the itinerary $\mathsf{LLL}\ldots$, which we denote $\overline{\mathsf{L}}$. This gives us the sequence of intervals

$$\mathsf{L}, \mathsf{LL}, \mathsf{LLL}, \cdots = \{[0, \tfrac{1}{2}], [0, \tfrac{1}{4}], [0, \tfrac{1}{8}], \ldots\}.$$

The intersection of this sequence of intervals is the set $\{0\}$. So $\overline{\mathsf{L}}$ is the itinerary of the point 0.

Consider the itinerary $\overline{\mathsf{R}}$. We refer to Figure 1.2.2 and see that this gives us the sequence of intervals

$$\mathsf{R}, \mathsf{RR}, \mathsf{RRR}, \cdots = \{[\tfrac{1}{2}, 1], [\tfrac{1}{2}, \tfrac{3}{4}], [\tfrac{5}{8}, \tfrac{3}{4}], [\tfrac{5}{8}, \tfrac{11}{16}], \dots\}.$$

It is harder to see, but this sequence of intervals converges to $\frac{2}{3}$.

Consider the itinerary $\mathsf{LR}\overline{\mathsf{L}}$. We refer to Figure 1.2.2 and see that this gives us the sequence of intervals

$$\mathsf{L}, \mathsf{LR}, \mathsf{LRL}, \mathsf{LRLL} \cdots = \{[0, \tfrac{1}{2}], [\tfrac{1}{4}, \tfrac{1}{2}], [\tfrac{3}{8}, \tfrac{1}{2}], [\tfrac{7}{16}, \tfrac{1}{2}], \dots\}.$$

The intersection of this sequence is $\{\frac{1}{2}\}$. Now consider the itinerary $\mathsf{RRL}\overline{\mathsf{L}}$. Again using Figure 1.2.2 we get

$$\mathsf{R}, \mathsf{RR}, \mathsf{RRL}, \mathsf{RRLL}, \cdots = \{[\tfrac{1}{2}, 1], [\tfrac{1}{2}, \tfrac{3}{4}], [\tfrac{1}{2}, \tfrac{5}{8}], [\tfrac{1}{2}, \tfrac{7}{16}], \dots\}.$$

The intersection of this sequence is also $\{\frac{1}{2}\}$. ◊

This last part of Example 1.2.8 shows how a single point can have multiple itineraries as we mentioned above. This happens because $\frac{1}{2}$ belongs in both L and R. We can similarly find multiple itineraries for points like $\frac{1}{4}, \frac{3}{4}, \frac{1}{8}$ and so forth. Points with multiple itineraries are always on the borders of our partitions from Figure 1.2.2.

The way to go from an itinerary to a point in $[0, 1]$ is called a Mealy automaton.

Example 1.2.9. The following represents a Mealy automaton for the Tent Map:

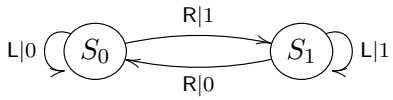

This graph translates between itineraries for the tent map from Example 1.2.1 and binary representations of numbers in $[0, 1]$. It works as follows:

We start in the state S_0 where L goes to 0, and R goes to 1. In S_1, R goes to 0 and L goes to 1. Whenever we send an R to either 0 or 1, we switch states. Here are a few

examples:

$$\mathsf{LL}\overline{\mathsf{L}} = 0.00\overline{0}$$

$$\mathsf{RR}\overline{\mathsf{L}} = 0.100\overline{0} = \tfrac{1}{2}$$

$$\mathsf{RL}\overline{\mathsf{L}} = 0.11\overline{1} = 1$$

$$\mathsf{RR}\overline{\mathsf{R}} = 0.10\overline{10} = \tfrac{2}{3}$$

The last one confirms the nested intervals calculation we did in Example 1.2.8.

In the next section we will rigorously define the notion of a Mealy automaton and point out this one is equivalent to something called a coding map.

1.3 Symbolic Dynamics

In this section we will use Section 6.5 in [2], [13], and [14] to build the ideas from Section 1.2 into rigorous definitions and theorems. Specifically, we must extend everything to the Riemann sphere so that we can use it in our case. We invite the reader to move freely between Section 1.2 and this one in an effort to see the concepts described here at work for the Tent Map.

Before we begin, the reader should make sure that they are familiar with the basic topological definitions of interior, closure, and quotient maps. They can all be found in [14]. The first two can be found in Section 17, while the last is in Section 22.

Definition 1.3.1. Let X be a topological space. A finite collection $\{\mathsf{P}_1, \ldots, \mathsf{P}_n\}$ of subsets of X is called a **topological partition** of X if

1. Each P_i is the closure of its interior.

2. The interiors of P_i and P_j are disjoint for all i and j.

3. The union $\mathsf{P}_1 \cup \mathsf{P}_2 \cup \cdots \cup \mathsf{P}_n = X$.

△

Definition 1.3.2. Let X be a compact metric space, let $\{\mathsf{P}_1, \ldots, \mathsf{P}_n\}$ be a topological partition of X, and let $\phi\colon X \to X$ be a function. We say that X has the **Markov property** with respect to ϕ if for every pair $i, j \in \{1, \ldots, n\}$ we have $\phi(\mathsf{P}_i) \cap \mathrm{Int}(\mathsf{P}_j) = \emptyset$ or $\mathsf{P}_j \subseteq \phi(\mathsf{P}_i)$. △

Definition 1.3.3. Let X be a compact metric space. Let $\{\mathsf{P}_1, \ldots, \mathsf{P}_n\}$ be a topological partition of X that has the Markov property with respect to the function ϕ. A **transition graph** is a graph with a vertex for each P_i and an oriented edge $\mathsf{P}_i \to \mathsf{P}_j$ if $\mathsf{P}_j \subseteq \phi(\mathsf{P}_i)$ for every $i, j \in \{0, \ldots, n\}$. △

Example 1.3.4. Let ϕ be the Tent Map. The following is a transition graph for the Tent Map:

It shows which symbols (and thus the intervals they represent) map to which other symbols under ϕ. Since, $\phi(\mathsf{L}) = \phi(\mathsf{R}) = [0, 1]$ we can see that both R and L map to both themselves and to each other. This means that *every* symbol sequence in L's and R's is an itinerary. This is not always the case, but makes for a very pretty and symmetric transition graph.

◊

Definition 1.3.5. Let G be a transition graph. Then the **symbol space** Ω_{dyn} associated with G is the set of all infinite sequences of P_i obtained by tracing out a path of infinite length on the transition graph. (It is so called because we denote the sets in the topological partition by symbols such as $\mathsf{P}_1, \mathsf{P}_7$, etc.). △

Note that Ω_{dyn} is trivially homeomorphic to a closed subset of $\{0, \ldots, n\}^\infty$. Thus, Ω_{dyn} is also homeomorphic to the Cantor set.

There is a **shift map** $\phi_{\text{dyn}}\colon \Omega_{\text{dyn}} \to \Omega_{\text{dyn}}$ defined by simply dropping the first symbol and shifting everything else one place to the left. The pair $(\Omega_{\text{dyn}}, \phi_{\text{dyn}})$ is often called a **subshift of finite type** in the literature.

We call an element of Ω_{dyn} an **itinerary**. A **finite itinerary** is a sequence of symbols obtained by tracing a finite path on G. Regardless of all this new terminology, given an itinerary $\mathsf{S}_0\mathsf{S}_1\ldots \in \Omega_{\text{dyn}}$ and a point $p \in X$, we can still determine if they correspond, just as we did for the tent map. If $\phi^{\circ k} \in \mathsf{S}_k$ for all k, then $\Pi(\mathsf{S}_0\mathsf{S}_1\ldots) = p$. Also, a finite itinerary still corresponds to the set of points whose itinerary begins with that finite string.

We now combine our all of these into the main definition that we'll need.

Definition 1.3.6. Let X be a compact metric space and let ϕ be a function on X. The topological partition $\{\mathsf{P}_1, \ldots, \mathsf{P}_n\}$ is called a **Markov partition** for ϕ if it has the Markov property with respect to ϕ and every itinerary in the symbol space Ω_{dyn} corresponds to a single point in X. △

The map which takes itineraries to points is called the **coding map** and is denoted $\Pi\colon \Omega_{\text{dyn}} \to X$. Note that Π is a quotient map in the usual topological sense. With all of this notation, we can draw the commutative diagram:

$$\begin{array}{ccc} \Omega_{\text{dyn}} & \xrightarrow{\phi_{\text{dyn}}} & \Omega_{\text{dyn}} \\ \Big\downarrow{\scriptstyle \Pi} & & \Big\downarrow{\scriptstyle \Pi} \\ J(\phi) & \xrightarrow{\phi} & J(\phi) \end{array}$$

Example 1.3.7. Let $\phi\colon [0,1] \to [0,1]$ be defined by the following

$$\phi(x) = \begin{cases} 2x + \frac{1}{2} & x \leq \frac{1}{4} \\ -x + 1\frac{1}{4} & \frac{1}{4} \leq x \leq \frac{1}{2} \\ -2x + 1\frac{3}{4} & \frac{1}{2} \leq x \leq \frac{3}{4} \\ -x + 1 & \frac{3}{4} \leq x \leq 1 \end{cases}.$$

Figure 1.3.1: A Graph of $\phi(z)$.

The graph of ϕ appears in Figure 1.3.1 As with our tent map example, we have a clear choice of how choose our topological partition and thus assign symbols to intervals in our domain. We will assign I to $[0, \frac{1}{4}]$, J to $[\frac{1}{4}, \frac{1}{2}]$, K to $[\frac{1}{2}, \frac{3}{4}]$, and L to $[\frac{3}{4}, 1]$.

Using Figure 1.3.1 we will construct the transition graph. We look at the first interval in the domain I and note that it maps to both the K and L intervals. We draw vertices for all three of these in our transition graph and mark a directed edge from I to each of the other two. Then we note that the J interval maps to the L interval only, so we draw in the J vertex with a directed edge to the L vertex. The K interval maps to itself and to J, so we add the corresponding directed edges. Finally, L maps to I only so we draw our final edge. The full transition graph is:

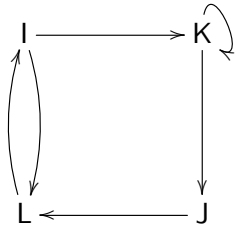

Following this transition graph along its directed edges gives us a sequence of symbols that is an itinerary for a point in $[0, 1]$. Thus we can have $\overline{\mathsf{K}}$, $\mathsf{KJ}\overline{\mathsf{LI}}$, or $\overline{\mathsf{IKJL}}$ but we could

never get $\overline{\mathsf{J}}$ or $\overline{\mathsf{KI}}$. We have not shown that $\{\mathsf{I}, \mathsf{J}, \mathsf{K}, \mathsf{L}\}$ is a Markov partition, but it is, and each of these itineraries corresponds to a specific point.

Let p_1 be the point with itinerary $\overline{\mathsf{K}}$ Since $\phi^{\circ k}(p_0) \in \mathsf{K}$ for all $k \in \mathbb{N}$, p_0 must be the solution to the equation $-2x + 1\frac{3}{4} = x$. So $p_0 = \frac{7}{12}$. We will also find the 2-cycle consisting of $\overline{\mathsf{IL}}$ and $\overline{\mathsf{LI}}$. For some $p_1 \in \mathsf{I}$, we know that $\phi^{\circ k}(p_1) = p_1$ for even k and that $\phi(p_1) \in \mathsf{L}$. In particular we have

$$\begin{aligned}\phi^{\circ 2}(p_1) =& \phi(2p_1 + \tfrac{1}{2}) \\ &= -(2p_1 + \tfrac{1}{2}) + 1 \\ &= -2p_1 + \tfrac{1}{2} \\ &= p_1\end{aligned}$$

Thus $p_1 = \frac{1}{6}$ and the other point in the 2-cycle is $\phi(\frac{1}{6}) = \frac{5}{6}$. We could also find cycles of greater length. (The only one missing is 3.) ◊

All of this is wonderful so far. We know what kind of partition we need, we know how build a transition graph, we know which itineraries are allowed, and we know that every itinerary specifies a single point. The question still remains: how do we know when the topological partition we have is in fact a Markov partition?

Definition 1.3.8. Let $X \in \mathbb{R}^n$ and let $U \supseteq X$ be open. Let $\phi \colon U \longrightarrow \mathbb{R}^n$ be a C^1 function and suppose $\phi(X) = X$. The function ϕ is **expanding** on X if there exists $k \in \mathbb{N}$ such that

$$||D_x\phi^{\circ k}(\mathbf{v})|| > ||\mathbf{v}||$$

for all $x \in X$ and non-zero $\mathbf{v} \in \mathbb{R}^n$. △

The D above is the standard derivative matrix. For our case in the complex plane, ϕ will be expanding whenever there exists some $k \in \mathbb{N}$ such that $|(\phi^{\circ k})'(z)| > 1$ for all $z \in X$.

Now we now have the following theorem from [3].

Theorem 1.3.9. *Let $X \subset \mathbb{R}^n$ be compact, let $U \supseteq X$ be open, and let $\phi\colon U \longrightarrow \mathbb{R}^n$ be a C^1 function such that $\phi(X) = X$. Let $\{\mathsf{P}_1, \ldots, \mathsf{P}_m\}$ be a topological partition of X with the Markov property, and suppose that:*

1. *The function ϕ is expanding on X and is one-to-one on each P_i, and*
2. *Each P_i is connected.*

Then $\{\mathsf{P}_1, \ldots, \mathsf{P}_m\}$ is a Markov partition.

Although we will not provide proof for these criterion, the intuition is similar to the tent map case from Proposition 1.2.7. If we have an itinerary $\mathsf{P}_1\mathsf{P}_2\ldots$, we can look at the sequence of finite subitineraries

$$\mathsf{P}_1,\ \mathsf{P}_1\mathsf{P}_2,\ \mathsf{P}_1\mathsf{P}_2\mathsf{P}_3, \ldots$$

For the itinerary to specify a unique point, these must be "shrinking". The set $\mathsf{P}_1\mathsf{P}_2$ is all the points of P_1 that map to P_2, so it is contained in the inverse image $\phi^{-1}(\mathsf{P}_2)$. Similarly, $\mathsf{P}_1\mathsf{P}_2\mathsf{P}_3 \subseteq \phi^{-2}(\mathsf{P}_3)$. This is where the expanding criteria comes in. Since ϕ is expanding, its inverse is "shrinking" the sequence of sets in each successive n iterations. By the time we get to infinity, ϕ^{-1} has shrunk the sets down to a single point.

The final concept we wish to introduce here is that of a **Mealy machine** or **Mealy automaton** from [15]. A Mealy automaton is a kind of function that converts a long string into another, one symbol at a time. For any element in the string the output depends not only on that current input, but also on the previous inputs. Mealy automata are often given as a way to specify the coding map Π and translate between itineraries in Ω_{dyn} and the state space X.

Definition 1.3.10. A **Mealy automaton** is a 6-tuple $\Sigma = (S, S_0, \Omega_{\text{in}}, \Omega_{\text{out}}, T, G)$ consisting of

- a finite set of states S

- a start state S_0
- a finite set of input symbols $\Omega_{\text{in}} = \{\mathsf{P}_1, \mathsf{P}_2, \ldots, \mathsf{P}_m\}$
- a finite set of output symbols $\Omega_{\text{out}} = \{\mathsf{X}_1, \mathsf{X}_2, \ldots, \mathsf{X}_k\}$
- a transition function $T\colon \Omega_{\text{in}} \times S \to S$
- an output function $G\colon S \times \Omega_{\text{in}} \to \Omega_{\text{out}}$.

△

We represent a Mealy automaton by a graph with directed, labeled edges. Each vertex represents a state, with one marked as the start state. From each vertex we have a directed edge to another state for each symbol in Ω_{in}. Thus the set of edges defines the transition function T. Each edge is labeled with both an input and an output. Thus the set of edges also defines the output function G. When we feed this machine the first element p_0 of a string, we follow the directed edge corresponding to p_0 away from the start state and record the output of that edge. Now we are in a new state S_1. From S_1, we follow the directed edge corresponding to the second element of the string p_1; record the output and repeat until we have converted the entire string.

See Example 1.2.9 for a Mealy automaton that represents the coding map of the Tent Map. Here, there are only two states S_0 and S_1. The set of input symbols is a set of symbols representing the topological partition $\{\mathsf{L}, \mathsf{R}\}$. The output symbols are $0, 1$ because we are expecting our output to be a binary number. On each edge we use the notation input | output.

1.4 Julia Sets

Given a complex function $\phi\colon \mathbb{C} \to \mathbb{C}$ we can construct its Julia set. In this chapter we will give a simple definition of Julia set for polynomial functions to build the readers intuition.

Then give a more difficult but rigorous definition for rational functions. Finally, we will give a definition of the Bubble Bath Julia set, which is the main object that we examine in this project.

For the first definition, the reader should recall the Stability Test and attracting basin from the end of Section 1.1.

Definition 1.4.1. Let $\phi : \mathbb{C} \to \mathbb{C}$ be a polynomial function. The **filled Julia set** for ϕ is the set of all points x whose orbit remains bounded. The **Julia set** for ϕ is the topological boundary of the filled Julia set. We use the notation $J(\phi)$ for both, depending on context. (In fact, for rational functions, they are the same.) △

Example 1.4.2. Let $\phi(z) = z^2$. Let $z_0 \in \mathbb{C}$. If $|z_0| \leq 1$, then $|f(z_0)| = |z^2| \leq 1$ and z_0 never approaches ∞. Thus the closed unit disc centered at the origin is in the filled Julia set $J(\phi)$. When $|z_0| > 1$, then $|f(z_0)| > 1$ and in fact, the orbit will diverge to ∞. Thus, the points with $|z_0| = 1$ – i.e. those of the unit circle – are exactly the boundary of the filled Julia set. So the (unfilled) Julia set is the unit circle. In Figure 1.4.1, we have a visual representation of the Julia set. The black is the filled Julia set, while the blue is not in the Julia set. The lighter blue is closer to the Julia set. We have plotted a few points in the orbits of $.96 + .06i$ in green and of $1.025 + .075i$ in red. ◊

Example 1.4.3. Let $\phi(z) = z^2 - 1$. The Julia set for ϕ is quite famous and is called the **Basilica**. The study of its homeomorphism group by Belk and Forrest is the main inspiration of this project. Once the reader comes to understand its dynamical structure here, they may like to examine Section 1.6 where we discuss Belk and Forrest's paper.

The function ϕ has a 2-cycle consisting of $\{-1, 0\}$. Thus both of these points will be in the filled Julia set. Also, any pre-images of these points, such as $1, \sqrt{2}$, and $-\sqrt{2}$, will also be in $J(\phi)$. In fact, any point whose orbit eventually hits this 2-cycle will be in $J(\phi)$. This

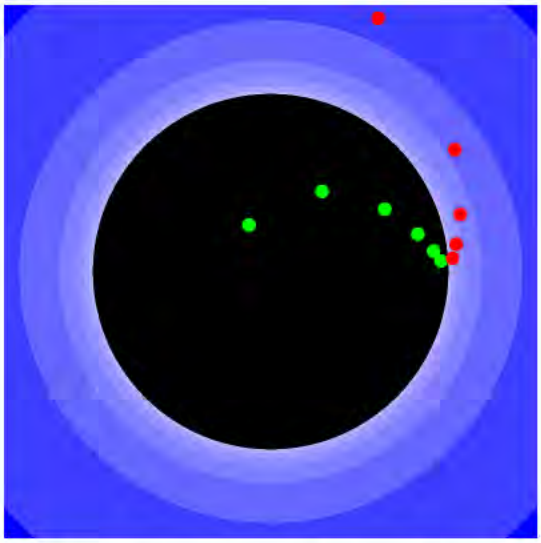

Figure 1.4.1: The filled Julia Set for $\phi(z) = z^2$ with the orbits of $1.025+.075i$, and $.96+.06i$.

is not, however, the complete Julia set. In fact, this 2-cycle is repelling, so there are some points which bounce around in $J(\phi)$ without ever hitting -1 or 0.

See Figure 1.4.2. ◊

The problem with our definition for Julia sets of polynomial functions lies in the fact that there is no clear notion of boundedness for rational complex functions on the Riemann sphere. However, we can call a point's orbit **bounded** if it does not converge to ∞. In other words, the Julia set consists of all the points not in the basin of attraction of ∞.

In this way we think of the Julia set as consisting of points that have very chaotic dynamics around them. The complement of the Julia set, also known as the Fatou set, contains points with very tame dynamics around them. In the polynomial case, the tamest orbits are those that are attracted to the fixed point ∞. The following definition states all of this rigorously, but obfuscates its meaning and is very difficult to use.

Definition 1.4.4. Let $\phi\colon \hat{\mathbb{C}} \to \hat{\mathbb{C}}$ be a non-constant holomorphic map. Let $\phi^{\circ k}$ be its k-fold iterate. Let $z_0 \in \hat{\mathbb{C}}$. If there exists a neighborhood U of z_0 so that every sequence of iterates $\{\phi^{\circ k_1}, \phi^{\circ k_2}, \dots\}$ restricted to U contains a subsequence which converges uniformly

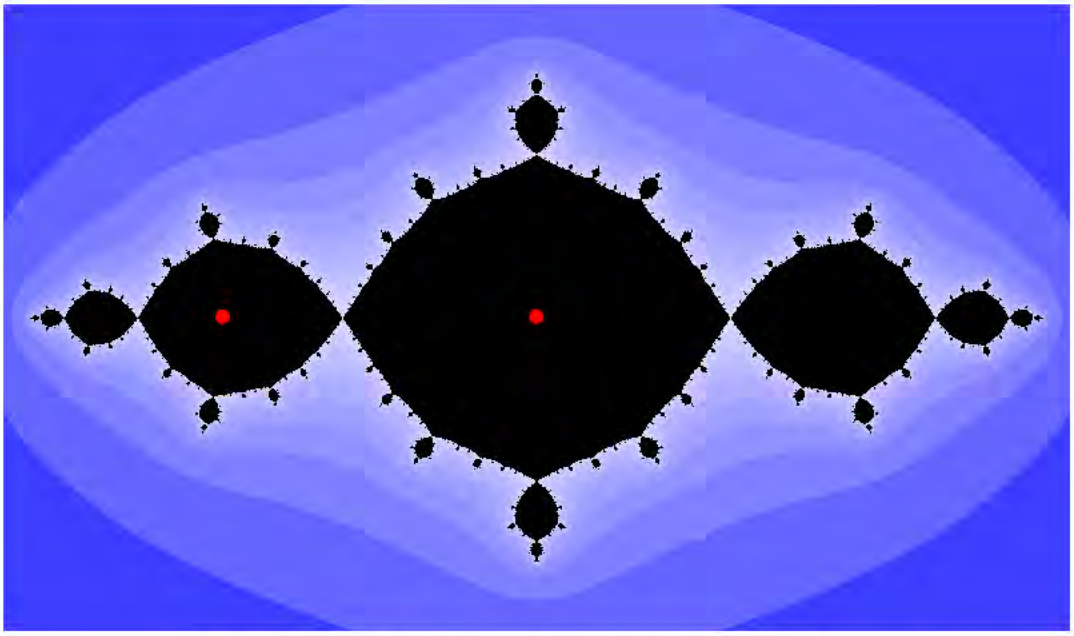

Figure 1.4.2: The filled Julia Set for $\phi(z) = z^2 - 1$. The points -1 and 0 appear in red.

on compact subsets of U to a continuous function, then we say that z_0 is in the **Fatou set** of ϕ. If no such neighborhood exists then we say that z_0 belongs to the **Julia set** $J(\phi)$ of ϕ. △

To unravel this definition somewhat we must refine our notion of attracting and repelling cycles. Recall that in Theorem 1.1.7 we considered the absolute value of the derivative of the k-fold iterate of ϕ at a point p_i in the cycle $\{p_1, p_2, \dots\}$. Now, for the case where ∞ is a point in a cycle, we consider the following limit

$$\lim_{p \longrightarrow \infty} \frac{1}{(\phi^{\circ k})'(p)} = \lim_{p \longrightarrow \infty} \frac{1}{\phi'(p)} \frac{1}{(\phi^2)'(p)} \cdots$$

Next, we have a theorem that is actually usable for determining some of the points of a Julia set.

Theorem 1.4.5. *The basin for every attracting cycle is contained in the Fatou set. The boundary of each basin is contained in the Julia set. Every repelling cycle is contained in the Julia set.*

We now include a number of lemmas and theorems from [13] without giving proof.

Lemma 1.4.6. *For any $k > 0$, the Julia set of the k-fold iterate $\phi^{\circ k}$ is equal to the Julia set of ϕ.*

The following are particularly relevant for our study of the function $\phi(z) = \frac{1-z^2}{z^2}$.

Lemma 1.4.7. *If ϕ is rational of degree two or more, then each of the following is true:*

1. *The Julia set of ϕ is non-empty.*
2. *The critical points of ϕ, if they exist, belong to the Fatou set.*
3. *The Julia set of ϕ has no isolated points.*

The last is in fact a corollary of the following theorem.

Theorem 1.4.8. *If $z_0 \in J(\phi)$, then the set of all iterated pre-images*

$$\{z \mid \phi^{\circ k}(z) = z_0 \text{ for some } k \geq 0\}$$

is everywhere dense in $J(\phi)$.

This last theorem gives insight into one method we used in our code for generating Julia set pictures. We start with any $z_0 \in J(\phi)$, compute all of its pre-images, then compute all pre-images of the pre-images, and so forth. Thus we can approach every point in the Julia set to arbitrary closeness.

Definition 1.4.9. A rational function ϕ is called **hyperbolic** if ϕ is expanding on its Julia set. △

This important theorem appears in Section 19 of [13].

Theorem 1.4.10. *A rational map ϕ of degree 2 or more is hyperbolic if and only if the orbit of every critical point converges to an attracting cycle.*

Corollary 1.4.11. *If ϕ is hyperbolic then every orbit in its Fatou set converges to an attracting cycle.*

With all of Milnor's theory at our disposal, we can finally give a definition of the Julia set for the function that we are interested in.

Proposition 1.4.12. *Let $\phi\colon \hat{\mathbb{C}} \to \hat{\mathbb{C}}$ be a function defined by $\phi(z) = \frac{1-z^2}{z^2}$ for all z in the Riemann sphere $\hat{\mathbb{C}}$. The Fatou set of ϕ is the basin of attraction of the 3-cycle consisting of the points $0, -1$, and ∞. The Julia set $J(\phi)$ is the set of points whose orbits are not attracted to the above 3-cycle.*

Proof. The derivative of ϕ is $\phi'(z) = \frac{-2}{z^3}$, so 0 and ∞ are the only critical points of ϕ. By Lemma 1.4.7 (2), they must be in the Fatou set. Note that $0, \infty, -1$ form the only attracting cycle. By Theorem 1.4.5, the entire basin of this 3-cycle must be in the Fatou set. Since 0 and ∞ are part of an attracting cycle, Theorem 1.4.10 implies that the basin is in fact the entire Fautou set. Then the complement of the basin is the Julia set so it is composed of exactly the points whose orbits do not converge to the three cycle. □

We call the Julia set $J(\phi)$ the **Bubble Bath** for its visual similarity to a tub of bubbles, see Figure 1.4.3. As with our previous images of Julia sets, the dark blue represents points in the Fatou set. Lighter shades of blue also represent points in the Fatou set, but they are closer to the Julia set. Unlike the previous Julia sets we have drawn, there is no black in Figure 1.4.3. This means that the Bubble Bath has no interior. (This is due to the fact that ϕ is rational.) In other words, the filled Julia set is equal to the Julia set. So the picture in Figure 1.4.4 is pretty good as well.

Figure 1.4.5 shows how ϕ acts on the Bubble Bath.

Also since ϕ is rational, it is important to remember that it is in fact defined on the whole Riemann sphere $\hat{\mathbb{C}}$. Figure 1.4.6 shows the Bubble Bath drawn on a sphere. In

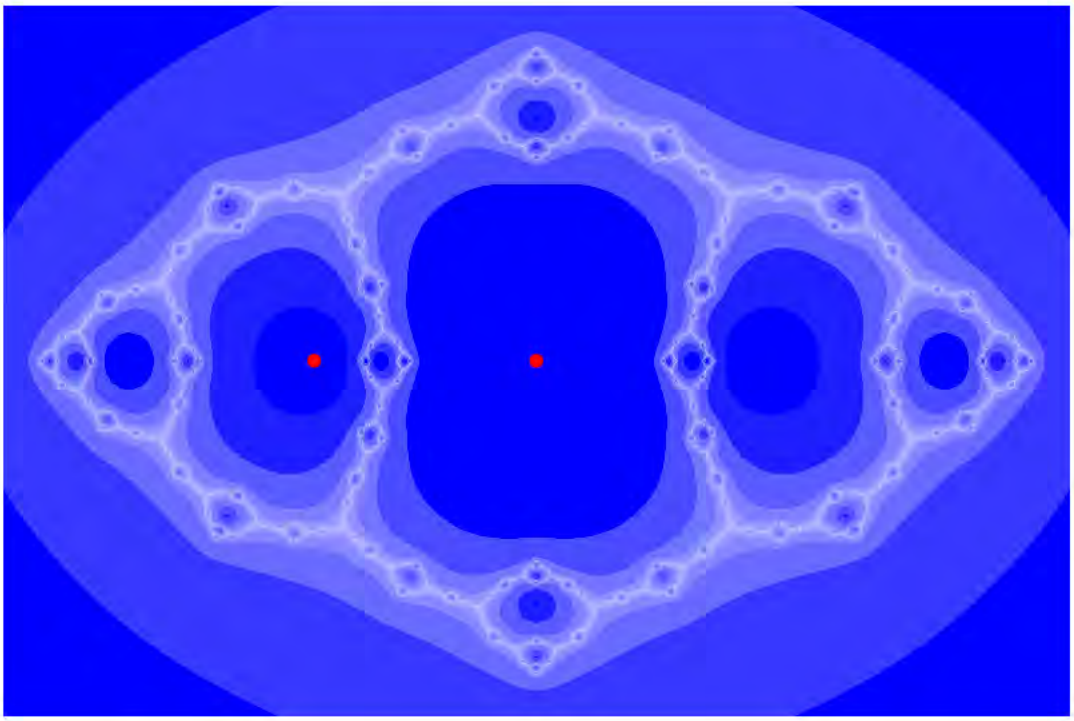

Figure 1.4.3: The Bubble Bath Julia set with 0 and -1 labeled in red.

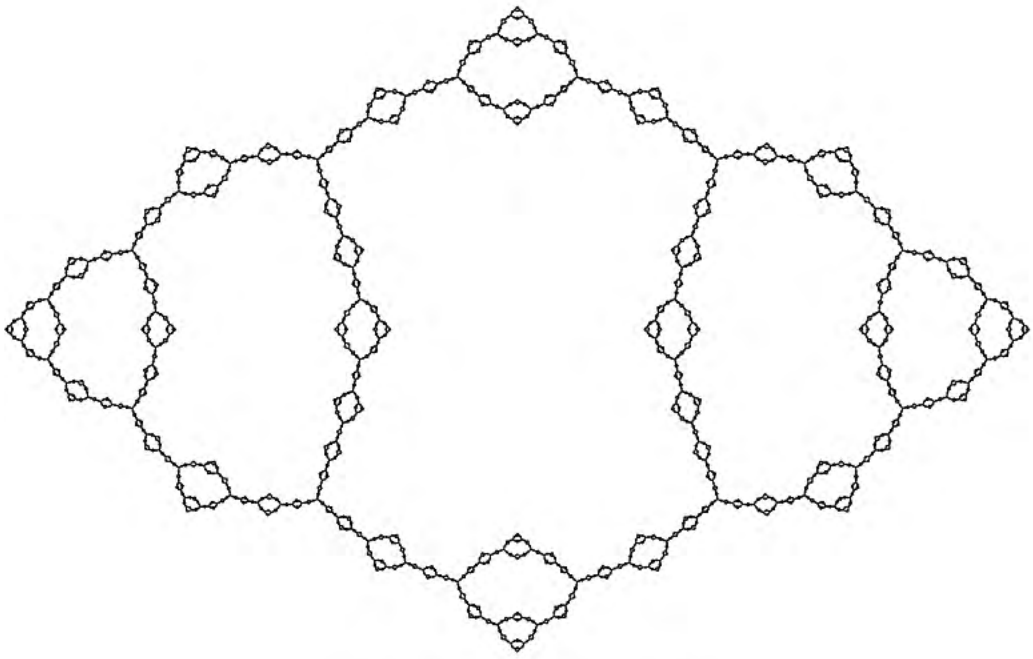

Figure 1.4.4: The Bubble Bath Julia set.

Figure 1.4.5: A visual representation of the function ϕ on the Julia set. Colors indicate which portions of the Julia set map to which.

Figure 1.4.3 we highlighted the points 0 and -1 by drawing them in red, but we could not draw ∞. On the sphere in Figure 1.4.6 we draw all three.

One last note about ϕ. Although Theorem 1.4.10 guarantees that ϕ is hyperbolic, we have also included Figure 1.4.7. This image shows a plot of the regions where ϕ is expanding as according to Definition 1.3.8. In particular, the blue shaded region represents all z such that $|(\phi^{\circ 3})'(z)| > 1$. The fact that ϕ is expanding on $J(\phi)$ is quite important. It not only means that ϕ is hyperbolic, but also plays a role in satisfying the criterion to determine a Markov partition. See Theorem 1.3.9.

1.5 Thompson's Group T

Here we will quickly introduce Thompson's group T. Consider the closed unit circle S^1 with points labeled by numbers in $[0, 1]$ rather than $[0, 2\pi]$. Divide S^1 into two pieces $[0, \frac{1}{2}]$ and $[\frac{1}{2}, 1]$ by making a simple cut at 0 and $\frac{1}{2}$.

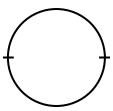

Then we cut each of these halves in half, and an assortment of the resulting halves get cut again.

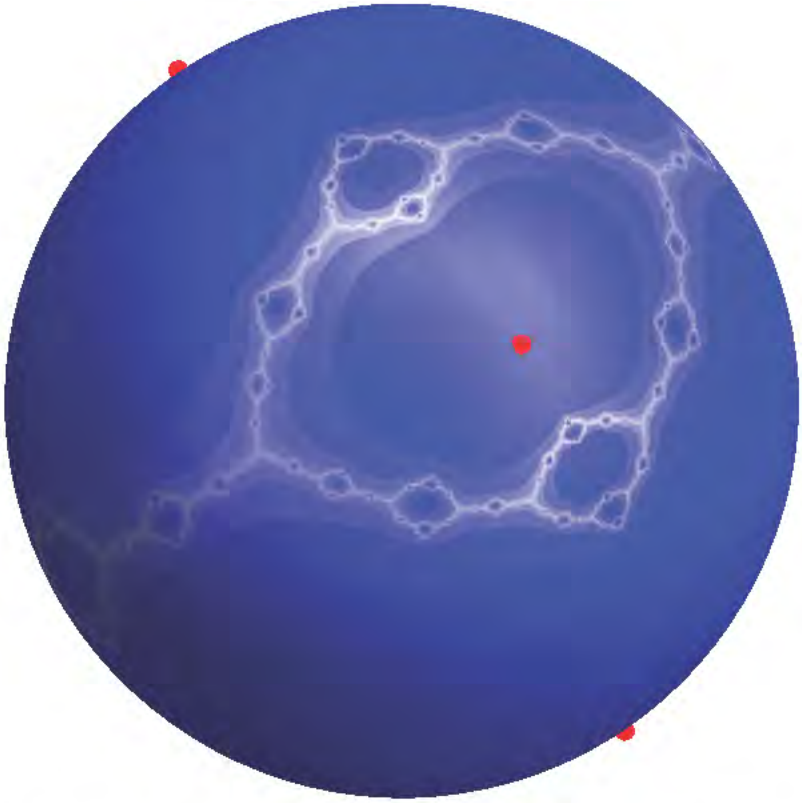

Figure 1.4.6: The Bubble Bath on the Riemann sphere with $0, \infty$, and -1 labeled in red.

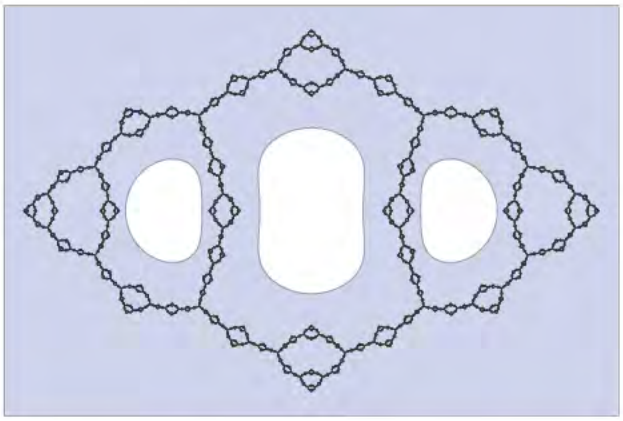

Figure 1.4.7: ϕ is expanding on the blue region, which contains the Bubble Bath.

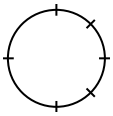

We now have a simple example of a **dyadic subdivision**. Any subdivision of the unit interval obtained from continuing this division process a finite number of times is a dyadic subdivision. The resulting **dyadic intervals** are all of the form $[\frac{k}{2^m}, \frac{k+1}{2^m}]$ for some $k \in \mathbb{Z}$ and $m \in \mathbb{N}$. Their endpoints are called **dyadic points**.

A **dyadic rearrangement** of S^1 is any piecewise-linear homeomorphism $f : S^1 \longrightarrow S^1$ such that the order of the intervals around the circle is preserved. There are three examples in Figure 1.5.1.

Lemma 1.5.1. *Let $f : S^1 \longrightarrow S^1$ be a piecewise-linear homeomorphism. Then f is a dyadic rearrangement if and only if it satisfies the following conditions:*

1. *The derivative of each linear segment of f has the form 2^m for some $m \in \mathbb{Z}$.*

2. *Each breakpoint of f maps a dyadic point in the domain to a dyadic point in the range.*

We can compose dyadic rearrangements with different numbers of breakpoints by adding additional (and previously unnecessary) cuts to the rearrangement with less breakpoints. In this manner the set of dyadic rearrangements of S^1 form a group known as **Thompson's Group** T.

Theorem 1.5.2.

1. *T is generated by the elements x_0, x_1 and δ shown in Figure 1.5.1.*

2. *T is simple.*

3. *T acts transitively on dyadic points on the circle.*

Figure 1.5.1: Generators for Thompson's group T.

We also want to mention the similar group F generated by x_0 an x_1. F is made up of all the elements of T which fix the point 0, in other words F is the group of dyadic rearrangements of the interval. For proof or more information on Thompson's groups, see [9] and [6].

1.6 The Basilica and its Group

In this section we will give a brief overview of the techniques and results in [4]. After introducing Thompson's group T and the Basilica Julia set for the function $\phi(z) = z^2 - 1$, see Example 1.4.3, Belk and Forrest use a homeomorphism from the unit circle to the Basilica to construct a convenient addressing system for points of the Basilica.

Theorem 1.6.1. *Let S^1 be the unit circle and let $J(\phi)$ be the Basilica. There exists a quotient map ψ such that the following diagram commutes.*

$$\begin{array}{ccc} S^1 & \xrightarrow{z^2} & S^1 \\ \downarrow{\scriptstyle \psi} & & \downarrow{\scriptstyle \psi} \\ J(\phi) & \xrightarrow[\phi]{} & J(\phi) \end{array}$$

Figure 1.6.1: External angles on the Basilica Julia set for $\phi(z) = z^2 - 1$.

We have a similar homeomorphism for the Bubble Bath called the Böttcher map which we will define in Section 2.1. For now, our main goal is to explain how a quotient map of this kind works, not provide proof. For a rigorous discussion of the following process, see Section 2 in [4].

Since 0 is a critical point, the points near zero are rotated by ϕ. By applying ϕ to a point p in a neighborhood of 0, it is rotated around 0 and then translated into a neighborhood of -1. As we zoom out from the origin, the translation becomes less and less significant.

For points in $\mathbb{C}$ far from the origin, ϕ is quite similar to the function $g(z) = z^2$. As $|z|$ grows, the -1 part of ϕ is dominated by z^2. Geometrically, g doubles angles and squares moduli. Thus g maps a line from the origin at angle θ to a line at angle 2θ. Our function ϕ has rays that it acts on in the same way. Far from the origin these look just like the lines for g. See Figure 1.6.1.

Example 1.6.2. Consider the positive real line greater than 2. This ray maps to itself, so it should be the angle 0 ray (there really is no other sensible choice anyways). The ray

made up of real numbers less than -2 maps to real numbers greater than 2. Thus, it will be the angle $\frac{1}{2}$ ray (we have identified the unit circle with $\mathbb{R}/\mathbb{Z}$ as in Section 1.5). $\Diamond$

Using these two rays we can begin to label other ϕ-rays with angles. Each ray hits the Basilica at a single point. When we have labeled a ray of every angle, we have the map ψ between the Basilica and the unit circle.

Next, Belk and Forrest define functions on these angles that all correspond to dyadic rearrangements of the circle. They introduce a visual tool called an **arc pair diagram** which serves the purpose of the images in Figure 1.5.1. Later we will have similar diagrams which we call **bubble diagram pairs**.

In Section 5, they define their group T_B, making heavy use of arc pair diagrams. The main purpose of Section 6 is to prove that T_B contains an isomorphic copy of T. In particular, they prove that the subgroup of T_B which only acts on the central component of the Basilica is isomorphic to T.

In Section 7, they state the following theorem where the generators $\{\beta, \gamma, \delta\}$ generate their isomorphic copy of T.

Theorem 1.6.3. *The group T_B is generated by the elements $\{\alpha, \beta, \gamma, \delta\}$*

This extra element α shifts each component of the Basilica to the right. Thus, we can get a copy of T on *any* component of the Basilica. In fact, the first lemma to help prove this theorem states that the four generators act transitively on components of the Basilica. We will use a similar strategy in our proof of generation for Theorem 3.4.1. To prove the theorem, Belk and Forrest use their arc pair diagrams measure the complexity of some $f \in T_B$ and show how to simplify it.

In the last section, Belk and Forrest prove their main results about the simplicity of the commutator subgroup. They define a two-coloring of the Basilica and examine how their generators act on this two-coloring. As it turns out, the generators either fix or swap the

colors. This defines a homomorphism $\pi\colon T_B \to \mathbb{Z}/2\mathbb{Z}$. They use Schreier's Lemma to find a generating set for the $\ker \pi$ and prove that it is the commutator subgroup $[T_B, T_B]$.

Theorem 1.6.4. *The commutator subgroup $[T_B, T_B]$ is simple and generated by*

$$\{\beta, \gamma, \delta, \alpha\beta\alpha^{-1}, \alpha\gamma\alpha^{-1}, \alpha\delta\alpha^{-1}\}.$$

This generating set is two isomorphic copies of T; one on the central component as mentioned above, and one on the largest left component. Finally, they use an opaque technique called Epsteins double commutator trick to show that $[T_B, T_B]$ is simple. As a corollary, they note that $[T_B, T_B]$ must be the only non-trivial proper normal subgroup of T_B and thus that it is also the only non-trivial proper subgroup with finite index.

2
The Bubble Bath Julia Set

In the first section of this chapter, we give a Markov partition and corresponding symbol space Ω_{dyn} for $\phi(z) = \frac{1-z^2}{z^2}$. Next, we describe a separate, geometric address system Ω_{geom} which allows us to easily label every point of the Bubble Bath. At first, we prove very little about Ω_{geom} and the reader must work on faith until Section 2.3. However, Ω_{geom} is useful even as an unproven heuristic as it lends us an intuitive understanding of the structure of the Bubble Bath. Furthermore, it is essential because the external rays method from [4] cannot fully address the Bubble Bath – because ϕ is rational. The symbolic dynamics and geometric address system approach is necessary to even define a group on the Bubble Bath. It is good, then, that Section 2.3 contains a proof that Ω_{geom} can be made rigorous. In particular, we construct an automaton to translate between the itineraries Ω_{dyn} of Section 2.1 and the geometric addresses Ω_{geom} of Section 2.2. Moreover, we expect that applying this method to other rational Julia sets could prove fruitful.

2.1 Itineraries

Let $\phi\colon \hat{\mathbb{C}} \to \hat{\mathbb{C}}$ be the quadratic rational function defined by $\phi(z) = \frac{1-z^2}{z^2}$ for all $z \in \hat{\mathbb{C}}$. As in Section 1.4, we refer to the Julia set for ϕ as the Bubble Bath, see Figure 1.4.3. In Chapter 4 we will discuss why we chose this function, and how it relates to other degree two rational functions.

In this section, we will develop itineraries for points in the Bubble Bath. First, we must construct internal angles for the connected regions in the Fatou set (the compliment of the Bubble Bath). These will be similar to the external angles discussed in [4].

The idea is that in every bubble, the function ϕ gives rise to curves from that bubble's "center" to the points of the Bubble bath on the boundary of that bubble. These curves are analogous to the angle rays of a circle, just like the Basilica's external rays we discussed in Section 1.6. We will start with the middle bubble, whose center is 0, and then extend these to every connected region of the Fatou set. We will need a theorem from [13].

Theorem 2.1.1. *Let $f\colon \hat{\mathbb{C}} \to \hat{\mathbb{C}}$ be a holomorphic function, let $n \geq 2$, and let $a_n \in \mathbb{C} - \{0\}$ and $a_i \in \mathbb{C}$ for all $i > n$. Let D^2 be the open unit disc and let $g\colon D^2 \to D^2$ be the function defined by $g(z) = z^n$. Suppose that*

$$f(z) = a_n z^n + a_{n+1} z^{n+1} + \dots$$

Then there exists a neighborhood U of 0 and a holomorphic function $\mathscr{B}\colon U \to D^2$ such that the following diagram commutes:

$$\begin{array}{ccc} U & \xrightarrow{\phi} & U \\ {\scriptstyle \mathscr{B}}\downarrow & & \downarrow{\scriptstyle \mathscr{B}} \\ D^2 & \xrightarrow[z^4]{} & D^2 \end{array}$$

The map $\mathscr{B}$ is called the ***Böttcher Map****.*

Figure 2.1.1: The Böttcher Map $\mathscr{B}$ gives rise to internal angles in each bubble.

Since $\phi^{\circ 3}$ is holomorphic, we can find a power series for it. We have

$$\phi^{\circ 3}(z) = \frac{z^4(2 - 4z^2 + z^4)}{(1 - 2z^2)^2} = 2z^4 + 4z^6 + 9z^8 + 20z^{10} + 44z^{12} + 96z^{14} + O(z^{15}).$$

Since ϕ is a hyperbolic map, Section 19 in [13] allows us to choose the middle bubble as our open neighborhood U. Now Theorem 2.1.1 gives us a map $\mathscr{B}$ from the middle bubble to the open unit disc. We use this $\mathscr{B}$ to define the angle of a point in the middle bubble. See Figure 2.1.1. Let p be a point in the middle bubble. The the **internal angle** of p is $\arg \circ \mathscr{B}(p)$ where arg is the typical argument function on the complex numbers..

Example 2.1.2. Figure 2.1.1 shows a number of labeled rays in the middle bubble. Every point p on the $\frac{1}{3}$ ray has the property that $\arg \mathscr{B}(p) = \frac{1}{3}$. Similarly with the rays labeled $\frac{3}{4}$ and 0. ◊

Next, we want to extend our angles to every bubble of the Fatou set. Because 0 is part of an attracting 3-cycle, we can consider other bubbles as pre-images under ϕ of the middle bubble. Let p be a point in any bubble B. Let k be the least integer such that $\phi^{\circ k}(B)$ is the middle bubble. Then the **internal angle** of p is $\arg \circ \mathscr{B} \circ \phi^{\circ k}(p)$. Since ϕ is continuous, the border of every bubble must eventually map to the boundary of the middle bubble also. This fact will help us extend our angles to the Julia set.

Figure 2.1.2: A Markov partition of the Bubble Bath gives rise to a system of itineraries.

In Section 18 in [13], Milnor shows that these rays do in fact "land" on the Bubble Bath at a single point. In other words, the Böttcher map $\mathscr{B}$ extends to a map $\overline{\mathscr{B}}\colon U \longrightarrow D^2$ from the border of the middle bubble $U \subseteq J(\phi)$ to the unit circle D^2.

Definition 2.1.3. Let $p \in J(\phi)$ and let k be the least integer such that $\phi^{\circ k}(p)$ is on the boundary of the middle bubble. The **internal angle** of p is given by $\arg \circ \overline{\mathscr{B}} \circ \phi^{\circ k}(p)$. $\triangle$

These internal angles do not allow us to specify a unique point of the Bubble Bath. In fact, given an angle θ, there are an infinite number of points at θ because every bubble has an angle θ. Instead, we will use these angles to create a topological partition of the Riemann sphere and build a symbol space of itineraries for points in the Bubble Bath.

Let $\mathsf{A}, \mathsf{B}, \mathsf{C}, \mathsf{X}, \mathsf{Y}$ and Z be the subsets of $J(\phi)$ contained in the closed regions on the Riemann sphere as shown in Figure 2.1.2. Since each subset is closed and they only overlap

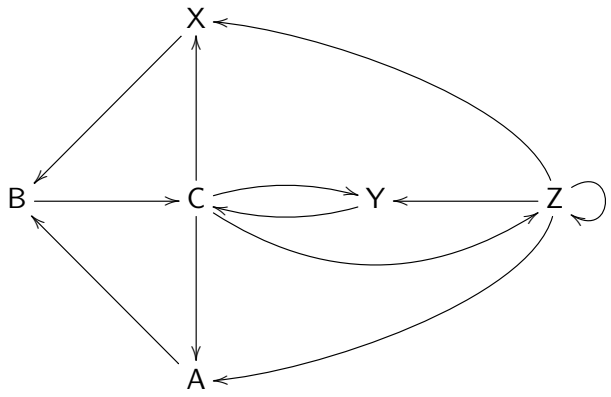

Figure 2.1.3: The transition graph for ϕ on the Markov partition $\{\mathsf{A}, \mathsf{B}, \mathsf{C}, \mathsf{X}, \mathsf{Y}, \mathsf{Z}\}$.

at their endpoints, it is clear that $\{\mathsf{A}, \mathsf{B}, \mathsf{C}, \mathsf{X}, \mathsf{Y}, \mathsf{Z}\}$ is a topological partition as according to Definition 1.3.1.

We chose these regions based on how ϕ maps $J(\phi)$ to itself, see Figure 1.4.5. Symbolically, ϕ maps each region as follows:

$$\phi(\mathsf{A}) = \mathsf{B}$$

$$\phi(\mathsf{B}) = \mathsf{C}$$

$$\phi(\mathsf{C}) = \mathsf{A} \cup \mathsf{Z} \cup \mathsf{Y} \cup \mathsf{X}$$

$$\phi(\mathsf{X}) = \mathsf{B}$$

$$\phi(\mathsf{Y}) = \mathsf{C}$$

$$\phi(\mathsf{Z}) = \mathsf{A} \cup \mathsf{Z} \cup \mathsf{Y} \cup \mathsf{X}.$$

Thus, $\{\mathsf{A}, \mathsf{B}, \mathsf{C}, \mathsf{X}, \mathsf{Y}, \mathsf{Z}\}$ has the Markov property with respect to ϕ. See Figure 2.1.3 for the corresponding transition graph.

Theorem 2.1.4. *The topological partition* $\{\mathsf{A}, \mathsf{B}, \mathsf{C}, \mathsf{X}, \mathsf{Y}, \mathsf{C}\}$ *is a Markov partition.*

Proof. We apply Theorem 1.3.9. By Theorem 1.4.10 (or Figure 1.4.7)we know that ϕ is hyperbolic, which means that it is expanding on $J(\phi)$. Note that ϕ is one-to-one on each

$\{\mathsf{A}, \mathsf{B}, \mathsf{C}, \mathsf{X}, \mathsf{Y}, \mathsf{C}\}$. Also, each region in $\{\mathsf{A}, \mathsf{B}, \mathsf{C}, \mathsf{X}, \mathsf{Y}, \mathsf{C}\}$ is connected. Thus the result is immediate. □

Definition 2.1.5. Let $\Omega_{\text{dyn}} \subset \{\mathsf{A}, \mathsf{B}, \mathsf{C}, \mathsf{X}, \mathsf{Y}, \mathsf{C}\}^{\infty}$ be the symbol space associated with the transition graph in Figure 2.1.3. Let $\phi_{\text{dyn}} : \Omega_{\text{dyn}} \to \Omega_{\text{dyn}}$ be the shift map on Ω_{dyn}. △

Let Π be the coding map, then the following diagram commutes:

$$\begin{array}{ccc} \Omega_{\text{dyn}} & \xrightarrow{\phi_{\text{dyn}}} & \Omega_{\text{dyn}} \\ \Pi \downarrow & & \downarrow \Pi \\ J(\phi) & \xrightarrow[\phi]{} & J(\phi) \end{array}$$

Now we provide a number of examples utilizing our new Markov partition and symbol space.

Example 2.1.6. Consider the point p_0 in A as it appears in Figure 2.1.4. An approximate value of p_0 is $0.990244i$. So an approximate orbit is

$$\{p_0, p_1, \dots\} = \{0.990244i, -2.0198, -0.754878, 0.754878, 0.754878, 0.754878 \dots\}$$

The points $p_1 = \phi(p_1)$ and $p_2 = \phi^{\circ 2}(p_0)$ and $p_3 = \phi^{\circ 3}(p_0)$ are also drawn in Figure 2.1.4. Observe that, in order, the points p_i are in regions $\mathsf{A}, \mathsf{Y}, \mathsf{C}$ and Z. Thus $\mathsf{AYCZ}\overline{\mathsf{Z}}$ is an itinerary for p_0. ◊

Example 2.1.7. In this example we'll find the point of a simple itinerary. After examining the transition graph in Figure 2.1.3, we note that there should be a point q_0 in a 2-cycle with itinerary $\overline{\mathsf{YC}}$. We solve the equation $\phi^{\circ 2}(q_0) = \frac{-1+2q_0^2}{(-1+q_0^2)^2} = q_0$ and get five solutions. One is the fixed point that the orbit of p_0 converged to. Two others are fixed points which we'll investigate next. This leaves -0.618034 and 1.61803. Since the latter is in Y, it must be that $q_0 = -0.618034$. In Figure 2.1.4 we have labeled both q_0 and q_1 in blue. The reader can imagine how the equation for a longer itinerary could be quite a bit more complicated. Still, since we are working with a Markov partition, it *is* possible. ◊

Figure 2.1.4: Three partial orbits on the Bubble Bath.

Example 2.1.8. The green points in Figure 2.1.4 are labeled such that $x_i = \phi^{\circ i}(x_0)$, just as the p_i's in Example 2.1.6. Since $x_0 \in \mathsf{C}$ and $x_1 \in \mathsf{Y}$, the itinerary of x_0 starts CY, but now we must make a choice because x_2 is in all of A, Z, and Y. We will also have to chose between B, C and X for the four symbol. In fact, because $\phi(x_3) = x_3$, our itinerary could end with an infinite number of B's, C's, or X's. $\lozenge$

The point x_3 from Example 2.1.8 is one of only four points that lie are on the boundary of the Markov partition $\{\mathsf{A}, \mathsf{B}, \mathsf{C}, \mathsf{X}, \mathsf{Y}, \mathsf{C}\}$. See Figure 2.1.2 and note that all four of them are at a place where three pieces of the Julia set intersect. The two on the left are fixed points of ϕ. Their numerical value is approximately $-0.877439 \pm 0.744862i$. We designate the one with positive imaginary part as the **upper fixed point** π_1 and the the other as the **lower fixed point** π_2. The two other points on the borders of the Markov partition map to π_1 and π_2.

Definition 2.1.9. A **triple point** is a point whose orbit converges to π_1 or to π_2.

With a little work we can use the continuity of ϕ to show that triple points are at points where three strands of the Bubble Bath come together. Further, we can show that that all such places are indeed triple points. Lastly, these triple points are dense in the Bubble Bath by Theorem 1.4.8. △

Since π_1 and π_2 are in three sets of $\{\mathsf{A}, \mathsf{B}, \mathsf{C}, \mathsf{X}, \mathsf{Y}, \mathsf{C}\}$, they have three itineraries. Since the orbit of every triple point eventually maps to one of the fixed points, every triple point has three itineraries.

2.2 Geometric Addresses

This section describes how we think about the symmetric structure of the Bubble Bath. This develops into another system of addressing points in the Bubble Bath – one different from itineraries. This address system is based in the visual geometry of the Bubble Bath, rather than the dynamics of ϕ. Consequently, it is much more understandable and a great deal easier to work with. Unfortunately, what we gain in intuition we lose in rigor, at least for now.

In reality, these addresses are poorly defined (at best) without proof involving dynamics. The geometric addresses should, by all rights, be defined in terms of itineraries. However, for now we push on ahead. The reader should simply be aware that none of what we describe is rigorous until we go through the long and tiresome proof in Section 2.3. Then we will see that the dynamical and geometric addresses are in fact equivalent.

The basic component of the Bubble Bath is a **strand** with a bubble in the middle. Every strand has four substrands, which are each themselves strands. The four substrands are the following:

1. the top - the piece above the bubble,

Figure 2.2.1: The Top, Left, Right, and Bottom substrands are colored in green, red, blue, and black respectively.

2. the bottom - the piece below the bubble,

3. the left - the left half of the bubble,

4. the right - the right half of the bubble.

See Figure 2.2.1. Some strands are horizontal, so we must choose an orientation. The piece of the strand that is "closer" to the upper fixed point π_1 is the top, while the piece that is closer to the lower fixed point π_2 is the bottom. This also defines which side of the bubble is the left, and which is the right. By "closer" we mean "has a shorter path contained in the Bubble Bath" (this is still not well defined because every path probably has infinite length, but the reader should interpret the previous sentence in the only way that makes sense).

Next we divide the Bubble Bath into three **main strands** from π_1 to π_2. We label the main strands i, j, and k as in Figure 2.2.2. We can now refer to every point in the Bubble

Figure 2.2.2: The **main strands** i, j, and k.

Bath by an address that starts with i, j, or k and is followed by an infinite sequence of T's, B's, L's, and R's - for Top, Bottom, Left, and Right.

Definition 2.2.1. The set of **geometric addresses** of points in the Bubble Bath is the set of letter sequences $\Omega_{\text{geom}} = \{i, j, k\} \times \{\mathsf{T}, \mathsf{B}, \mathsf{L}, \mathsf{R}\}^{\infty}$. △

Note that Ω_{geom} is a topological space with the product topology. It is homeomorphic to a Cantor set.

We can also give finitely many letters, this will determine a whole strand rather than a single point.

Definition 2.2.2. A set $S \subseteq J(\phi)$ is a **basic strand** if it is determined by a sequence of letters $\mu \in \{i, j, k\} \times \{\mathsf{T}, \mathsf{B}, \mathsf{L}, \mathsf{R}\}^n$ for some finite n. The **length** of μ and S is the total number of letters $n+1$. Every basic strand has **endpoints** given by the addresses $\mu\overline{\mathsf{T}}$ and $\mu\overline{\mathsf{B}}$. For convenience, we often use μ for both the strand and sequence of letters. △

Basic strands are connected components of the Bubble Bath contain every point between their endpoints and are completely contained in one of the main strands i, j, or k. If we look at all the strands of length n, that would give us a topological partition of the Bubble bath into basic strands.

Example 2.2.3. We have drawn and labeled some points in Figure 2.2.3. The point q is on the i strand, the bottom strand, the right component of the bottom strand's bubble, and infinitely many more right sections of bubbles after that. So the address for q is $i\mathsf{B}\overline{\mathsf{R}}$.

The point p is a triple point. An address for p is $k\mathsf{T}\overline{\mathsf{B}}$ because it is on the k strand, it is in the top section, it is at the bottom section of that, and infinitely many more bottom sections. Just as with itineraries, it is possible to label this triple point with two other addresses. We could label p as $k\mathsf{L}\overline{\mathsf{T}}$ by "approaching" it from the left section of the k strand. Similarly, we could replace the L with an R by approaching it from the right section of the i strand. The next definition states this idea for any triple point. ◊

Let p be a triple point. As described at the end of Example 2.2.3, each of p's addresses corresponds to "approaching" p from one of the strands that intersect at p. The choice of the standard cyclic order corresponds to ordering these three strands counterclockwise.

Definition 2.2.4. Let S be a basic strand besides the main strands with finite address ω. The **partner pair** of triple points of S are the points at the top and bottom of the main bubble of S. The addresses for the partner pair of S are as follows:

- the **top triple point** of S has the following three addresses

$$\omega\mathsf{T}\overline{\mathsf{B}}, \quad \omega\mathsf{L}\overline{\mathsf{T}}, \quad \omega\mathsf{R}\overline{\mathsf{T}}$$

- the **bottom triple point** has the following three addresses

$$\omega\mathsf{B}\overline{\mathsf{T}}, \quad \omega\mathsf{R}\overline{\mathsf{B}}, \quad \omega\mathsf{L}\overline{\mathsf{B}}.$$ △

Figure 2.2.3: The points q and p have geometric address $i\mathsf{B}\overline{\mathsf{R}}$ and $k\mathsf{T}\overline{\mathsf{B}}$ respectively.

Definition 2.2.5. Let p be a triple point other than π_1 and π_2. Then the **standard cyclic order** of p's three addresses is the ordering that we gave in Definition 2.2.4 with the additional condition that we consider the order to be cyclic. For π_1 the standard cyclic order is $(i\overline{\mathsf{T}}, j\overline{\mathsf{T}}, k\overline{\mathsf{T}})$ and for π_2 it is $(k\overline{\mathsf{B}}, j\overline{\mathsf{B}}, i\overline{\mathsf{B}})$. △

Claim 2.2.6. *Each geometric address in Ω_{geom} refers to a single point in the Bubble Bath.*

This claim can be only be proved with material in Section 2.3. Even with the proof, though, it can be hard to determine which point a sequence really refers to. Here are examples of some addresses where it is hard, and of some where it is easy.

Example 2.2.7. Let μ be a basic strand.

The geometric address $\mu\overline{\mathsf{R}}$ gives a sequence of strands that all contain the "smaller" stand to the right. These converge to the unique "rightmost" point of μ.

Similarly, the address $\mu\overline{\mathsf{L}}$ refers to the "leftmost" point of μ.

The addresses $\mu\overline{\mathsf{B}}$ refers to the bottom triple point of μ, one of the endpoints of μ.

Now consider $\mu\overline{\mathsf{RT}}$. It will certainly be on the top half of the right strand of μ. In fact, we can even determine its location within an arbitrarily small amount of accuracy. Still, it is very hard to tell what point these strands all have in common. $\Diamond$

Since we can refer to any point by an address, it is natural to define ϕ on the addresses. First, we need the flip operation.

Definition 2.2.8. Let $\mathsf{X}, \mathsf{Y} \in \Omega_{\text{geom}}$. Then the **flip operation** is defined by the following:

$$(\mathsf{XY})^* = \mathsf{X}^*\mathsf{Y}^*,$$

$$\mathsf{L}^* = \mathsf{R}, \quad \mathsf{R}^* = \mathsf{L}, \quad \mathsf{B}^* = \mathsf{T}, \quad \mathsf{T}^* = \mathsf{B},$$

$$\text{and} \quad i^* = i, \quad j^* = j, \quad k^* = k. \qquad \triangle$$

We can apply the flip operation to a point or set of points in the Bubble Bath. Let μ be basic strand, then the **flipped** strand (naturally) has address μ^*. The flip operation is so named because its geometry corresponds to rotating the μ by 180°, so that the partner pair of triple points switch places with each other and the endpoints switch places with each other.

Definition 2.2.9. Let

$$\phi_{\text{geom}} \colon \Omega_{\text{geom}} \to \Omega_{\text{geom}}$$

be the function given by the following equations and induction on the symbols of an arbitrary element $\mu \in \Omega_{\text{geom}}$:

$$\begin{array}{llll} \phi_{\text{geom}}(i\mu) = j\mu & \phi_{\text{geom}}(j\mu) = k\mu & & \\ \phi_{\text{geom}}(kT\mu) = i\mu & \phi_{\text{geom}}(kB\mu) = i\mu & \phi_{\text{geom}}(kR\mu) = j\mu^* & \phi_{\text{geom}}(kL\mu) = k\mu^*. \end{array}$$

Figure 1.4.5 shows a picture of ϕ_{geom}. $\triangle$

In the next section we will prove that this is indeed equivalent to the function ϕ on the Bubble Bath Julia set $J(\phi)$.

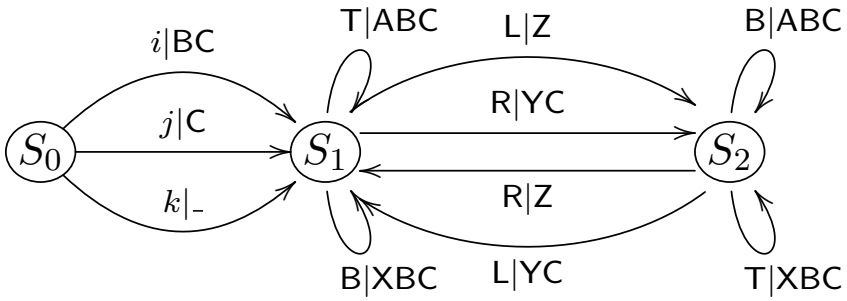

Figure 2.3.1: The automaton Σ is a function.

2.3 An Automaton Between the Two

We now have two ways to understand the structure of our Julia set. The first is rigorously defined by symbolic dynamics. It is a confusing mess of letters, but has rigorous mathematical meaning. The second is intuitive and easy to understand but is defined based on little more than observations from pictures about the Julia set's symmetries. Here we present a way to move between the two.

Let $\Sigma\colon \Omega_{\text{geom}} \longrightarrow \Omega_{\text{dyn}}$ be the Mealy automaton represented by Figure 2.3.1. Although Σ may at first seem complicated, we should point out that it is mostly symmetric. The state S_0 is only active once, for the starting strand i, j, or k. After that, states S_1 and S_2 have a similar structure, but send act oppositely. They send the same letters in Ω_{geom} to opposite symbols in Ω_{dyn}. We have a lemma below formalizing this relationship between states S_1 and S_2. Also, we should point out that the bottom arrow from S_0 has no output. When we have an itinerary that begins with k, this arrow contributes nothing to the new itinerary.

When we are doing computations with Σ, we must keep track of which state it is in. To this end, Σ will represent the start state, Σ_1 will represent S_1, and Σ_2 will represent S_3.

Lemma 2.3.1. *Let $\Sigma\colon \Omega_{\text{geom}} \longrightarrow \Omega_{\text{dyn}}$ be the Mealy automaton in Figure 2.3.1.*

Then $\Sigma_1(\omega^*) = \Sigma_2(\omega)$ *for all* $\omega \in \Omega_{\text{geom}}$.

Proof. Since $i^* = i$, $j^* = j$, and $k^* = k$, we can prove the equality for $\omega \in \{\mathsf{T}, \mathsf{B}, \mathsf{L}, \mathsf{R}\}^\infty$. Furthermore, since Σ is defined recursively, we only need to do it for each single symbol $\mathsf{T}, \mathsf{B}, \mathsf{L}$ and R.

1. Let $\omega = \mathsf{T}$. We have $\Sigma_2(\mathsf{T}) = \mathsf{XBC}$ and $\Sigma_1(\mathsf{T}^*) = \Sigma_1(\mathsf{B}) = \mathsf{XBC}$.

2. Let $\omega = \mathsf{B}$. We have $\Sigma_2(\mathsf{B}) = \mathsf{ABC}$ and $\Sigma_1(\mathsf{B}*) = \Sigma_1(\mathsf{T}) = \mathsf{ABC}$.

3. Let $\omega = \mathsf{L}$. We have $\Sigma_2(\mathsf{L}) = \mathsf{YC}$ and $\Sigma_1(\mathsf{L}^*) = \Sigma_1(\mathsf{R}) = \mathsf{YC}$.

4. Let $\omega = \mathsf{R}$. We have $\Sigma_2(\mathsf{R}) = \mathsf{Z}$ and $\Sigma_1(\mathsf{R}^*) = \Sigma_1(\mathsf{L}) = \mathsf{Z}$.

□

Theorem 2.3.2. *Let* Σ *be the Mealy automaton represented in Figure 2.3.1. Let* $\phi_{\text{dyn}} \colon \Omega_{\text{dyn}} \to \Omega_{\text{dyn}}$ *be the shift map. Let* $\phi_{\text{geom}} \colon \Omega_{\text{geom}} \to \Omega_{\text{geom}}$ *be the function* ϕ *on* Ω_{geom} *as in Definition 2.2.9.*

Then the following diagram commutes:

$$\begin{array}{ccc} \Omega_{\text{geom}} & \xrightarrow{\phi_{\text{geom}}} & \Omega_{\text{geom}} \\ \Big\downarrow{\scriptstyle \Sigma} & & \Big\downarrow{\scriptstyle \Sigma} \\ \Omega_{\text{dyn}} & \xrightarrow{\phi_{\text{dyn}}} & \Omega_{\text{dyn}} \end{array}$$

Proof. We want to show that $\Sigma \circ \phi_{\text{geom}} = \phi_{\text{dyn}} \circ \Sigma$. Let $\omega \in \Omega_{\text{geom}}$. We will need six cases where ω ranges through all the possible addresses in the domain of ϕ_{geom}. Please excuse the abuse of the symbol ω that follows.

1. Let $\omega = i\omega$. We have

$$\Sigma \circ \phi_{\text{geom}}(i\omega) = \Sigma(j\omega) = \mathsf{C}\Sigma_1(\omega), \text{ and}$$

$$\phi_{\text{dyn}} \circ \Sigma(i\omega) = \phi_{\text{dyn}}(\mathsf{BC}\Sigma_1(\omega)) = \mathsf{C}\Sigma_1(\omega).$$

2. Let $\omega = j\omega$. We have

$$\Sigma \circ \phi_{\text{geom}}(j\omega) = \Sigma(k\omega) = \Sigma_1(\omega), \text{ and}$$
$$\phi_{\text{dyn}} \circ \Sigma(j\omega) = \phi_{\text{dyn}}(\mathsf{C}\Sigma_1(\omega)) = \Sigma_1(\omega).$$

3. Let $\omega = k\mathsf{T}\omega$. We have

$$\Sigma \circ \phi_{\text{geom}}(k\mathsf{T}\omega) = \Sigma(i\omega) = \mathsf{BC}\Sigma_1(\omega), \text{ and}$$
$$\phi_{\text{dyn}} \circ \Sigma(k\mathsf{T}\omega) = \phi_{\text{dyn}}(\Sigma_1(\mathsf{T}\omega)) = \phi_{\text{dyn}}(\mathsf{ABC}\Sigma_1(\omega)) = \mathsf{BC}\Sigma_1(\omega).$$

4. Let $\omega = k\mathsf{B}\omega$. We have

$$\Sigma \circ \phi_{\text{geom}}(k\mathsf{B}\omega) = \Sigma(i\omega) = \mathsf{BC}\Sigma_1(\omega), \text{ and}$$
$$\phi_{\text{dyn}} \circ \Sigma(k\mathsf{B}\omega) = \phi_{\text{dyn}}(\Sigma_1(\mathsf{B}\omega)) = \phi_{\text{dyn}}(\mathsf{XBC}\Sigma_1(\omega)) = \mathsf{BC}\Sigma_1(\omega).$$

5. Let $\omega = k\mathsf{R}\omega$. We use Lemma 2.3.1 and have

$$\Sigma \circ \phi_{\text{geom}}(k\mathsf{R}\omega) = \Sigma(j\omega^*) = \mathsf{C}\Sigma_1(\omega^*) = \mathsf{C}\Sigma_2(\omega), \text{ and}$$
$$\phi_{\text{dyn}} \circ \Sigma(k\mathsf{R}\omega) = \phi_{\text{dyn}}(\Sigma_1(\mathsf{R}\omega)) = \phi_{\text{dyn}}(\mathsf{YC}\Sigma_2(\omega)) = \mathsf{C}\Sigma_2(\omega).$$

6. Let $\omega = k\mathsf{L}\omega$. Again we use Lemma 2.3.1

$$\Sigma \circ \phi_{\text{geom}}(k\mathsf{L}\omega) = \Sigma(k\omega^*) = \Sigma_1(\omega^*) = \Sigma_2(\omega), \text{ and}$$
$$\phi_{\text{dyn}} \circ \Sigma(k\mathsf{L}\omega) = \phi_{\text{dyn}}(\Sigma_1(\mathsf{L}\omega)) = \phi_{\text{dyn}}(\mathsf{Z}\Sigma_2(\omega)) = \Sigma_2(\omega).$$

□

Corollary 2.3.3. *Let* Π *be the coding map from Definition 1.3.6. Then with all the same notation as above, the following diagram commutes:*

$$\begin{array}{ccc} \Omega_{\text{geom}} & \xrightarrow{\phi_{\text{geom}}} & \Omega_{\text{geom}} \\ \Big\downarrow{\scriptstyle \Sigma} & & \Big\downarrow{\scriptstyle \Sigma} \\ \Omega_{\text{dyn}} & \xrightarrow{\phi_{\text{dyn}}} & \Omega_{\text{dyn}} \\ \Big\downarrow{\scriptstyle \Pi} & & \Big\downarrow{\scriptstyle \Pi} \\ J(\phi) & \xrightarrow{\phi} & J(\phi) \end{array}$$

This corollary is the main point of this entire section. With it, we know that all the properties of Ω_{geom} that we assumed were true in Section 2.2 *really do hold.*

Example 2.3.4. Consider the basic strand given by $k\mathsf{T}$. We note that $\Sigma(k\mathsf{T}) = \mathsf{ABC}$. The subset of $J(\phi)$ given by ABC really is the top substrand of the strand we call k.

The point $p \approx 0.26218 + 1.10736i$ had geometric address $k\mathsf{TL}\overline{\mathsf{B}}$. We compute

$$\Sigma(k\mathsf{TL}\overline{\mathsf{B}}) = \Sigma_1(\mathsf{TL}\overline{\mathsf{B}}) = \mathsf{ABC}\Sigma_1(\mathsf{L}\overline{\mathsf{B}}) = \mathsf{ABCZ}\Sigma_2(\overline{\mathsf{B}}) = \mathsf{ABCZ}\overline{\mathsf{ABC}}.$$

We have also computed an approximate partial orbit $\{0.26218 + 1.10736i, -1.69023 - 0.346245i, -0.691122 - 0.132091i, 0.877439 - 0.744862i, -0.877439 + 0.744862i\}$. We compare this to Figure 2.1.2 ad confirm that these points land in the appropriate sets of the Markov partition. $\Diamond$

Every definition we gave in Section 2.2 can be reformulated so that it is defined by Σ^{-1}. (The inverse of our Mealy automaton simply has the input and output reversed on its edges.) For instance, we could define $\Omega_{\text{geom}} := \Sigma^{-1}\Omega_{\text{dyn}}$.

Finally, we must point out that $\Pi \circ \Sigma$ is a quotient map in the usual topological sense.

3
A Thompson-Like Group for the Bubble Bath

This chapter contains our main results about the group for the Bubble Bath. Namely, that it contains a copy of Thompson's group T, that it is finitely generated by four elements, and that it has a simple subgroup of index-six.

In Section 3.1 we define our group T_{BB} of "piecewise-linear orientation preserving" homeomorphisms via the geometric addresses Ω_{geom}. In Section 3.2, we introduce a tool called a bubble diagram pair to visually represent the elements of T_{BB}. Section 3.3 defines the generators that we will work with and proves that there is a subgroup of T_{BB} that is isomorphic to T. Section 3.4 proves that T_{BB} is generated by four elements. In Section 3.5, we use a variety of methods from [4] to prove our simplicity result. First, we define a homomorphism $\rho\colon T_{BB} \to S_3$ based on a coloring of the Bubble Bath. We denote the kernel of ρ by K and note that it has index six. Then we make use of Scheier's Lemma to show that K is generated by six copies of T, each acting on different bubbles. We use a double commutator trick to show that K is simple and that every other normal subgroup of T_{BB} contains K. Finally, as corollaries we have a classification of the finite-index normal subgroups of T_{BB} and that K is the double commutator subgroup.

3.1 Piecewise-Linear Homeomorphisms

In this section we will define our group on the Bubble Bath. Since we are interested in some kind of analogue of Thompson's group T, elements of our group should somehow be "piecewise-linear" homeomorphisms. Furthermore, they should have a finite number of breakpoints that always occur on some predictable subset of the Bubble Bath, just as elements of T have breakpoints at dyadics.

In order to guarantee a finite number of breakpoints we will want to divide the Bubble Bath into a finite number of pieces. Naturally, each of these pieces should be a basic strand. We can use our notion of a topological partition from Definition 1.3.1.

Definition 3.1.1. Let $f_{\text{geom}} \colon \Omega_{\text{geom}} \to \Omega_{\text{geom}}$ be a function and let $n \in \mathbb{N}$. Let $\{\mu_i\}_{i=1}^n$ and $\{\lambda_i\}_{i=1}^n$ be sets of finite addresses μ_i and λ_i such that the basic strands represented by each are topological partitions of the Bubble Bath. We call f_{geom} a **piecewise-linear bijection** if for every $i \in \{1, \dots n\}$, there exists a unique $j \in \{1, \dots n\}$ so that one of the following **rules** holds:

- $f_{\text{geom}}(\mu_i\omega) = \lambda_j\omega$ for all $\omega \in \{\mathsf{T}, \mathsf{B}, \mathsf{L}, \mathsf{R}\}^\infty$
- $f_{\text{geom}}(\mu_i\omega) = \lambda_j\omega^*$ for all $\omega \in \{\mathsf{T}, \mathsf{B}, \mathsf{L}, \mathsf{R}\}^\infty$.

The **breakpoints** of f_{geom} are the points at the ends of the basic strands corresponding to $\{\mu_i\}_{i=1}^n$, where the rules defining f_{geom} change. △

Suppose f_{geom} is a piecewise-linear bijection. Is this enough to guarantee that f_{geom} descends to a well defined $f \colon J(\phi) \to J(\phi)$? We can see that such an f would only send basic strands to basic strands. Also, it would take finitely many rules to define it on the whole Bubble Bath. Between breakpoints, on the "interior" of each strand, f would be well defined. It would either map everything with the same orientation or it would flip the

entire strand. The breakpoints of f would be triple points, because the endpoint of every strand is a triple point.

These breakpoint triple points may give us trouble. Since a triple point $p \in J(\phi)$ has three addresses, it may belong to multiple strands. Thus, one rule of f_{geom} might send two addresses of p to two addresses which do not correspond to the same triple point. Thus the image $f(p)$ is not defined at all. In the next proposition, we show that requiring f_{geom} to map all three addresses for p to the "same place" will indeed allow it to descend (at least locally at p).

Proposition 3.1.2. *Let $f_{\text{geom}} \colon \Omega_{\text{geom}} \longrightarrow \Omega_{\text{geom}}$ be a piecewise-linear bijection. Suppose that for all triple points $p \in J(\phi)$ with addresses $\omega_1, \omega_2, \omega_3 \in \Omega_{\text{geom}}$ the three addresses $f_{\text{geom}}(\omega_1), f_{\text{geom}}(\omega_2), f_{\text{geom}}(\omega_3)$ define a single triple point q.*

Then f_{geom} descends to a homeomorphism $f \colon J(\phi) \longrightarrow J(\phi)$ and for all triple points p there exists a triple point q such that $f(p) = q$.

When this situation arrises, we say that f is a **piecewise-linear** homeomorphism.

Proof. Since f_{geom} is piecewise-linear, it will be continuous on Ω_{geom} under the product topology. See Corollary 2.3.3 and recall that $\Pi \circ \Sigma$ is a quotient map. Then f is well defined and continuous by Theorem 22.2 in [14]. Since f_{geom} is a bijection, so is f. Since $J(\phi)$ is compact and Hausdorff, f has a continuous inverse. □

Definition 3.1.3. Let $f \colon J(\phi) \longrightarrow J(\phi)$ be a piecewise-linear homeomorphism. We say that f is **orientation preserving** if it preserves the counterclockwise order of the strands that intersect at every triple point. △

We can use the standard cyclic order from Definition 2.2.5 to determine if f is orientation preserving.

Proposition 3.1.4. *Let f be a piecewise-linear homeomorphism. Then f is orientation preserving if and only if f_{geom} preserves the standard cyclic order of the addresses of every breakpoint.*

Proof. It would be trivial except that we would like f to preserve the counterclockwise order of strands at *all* triple points. We will give a (mostly) reversible proof.

Suppose that f is orientation preserving. Let f_{geom} be the piewise-linear bijection with the property from Proposition 3.1.2 that descends to f. Suppose p is a triple point. Thus p is on the interior of some basic strand given by μ_p in the domain of f_{geom} or it is on the edge of some of three basic strands μ_p, μ_q, and μ_r.

If the former is true, then p has the three addresses $\mu_p\omega_1, \mu_p\omega_2, \mu_p\omega_3$ for some choice of $\omega_i \in \{\mathsf{T}, \mathsf{B}, \mathsf{L}, \mathsf{R}\}^\infty$ as according to Definition 2.2.4. Now for all ω_i we have $f_{\text{geom}}(\mu_p\omega_i) = \mu\omega_i$ or $\mu\omega_i^*$ for some basic strand μ. Both of these preserve the standard cyclic order.

If the latter is true, we know that the basic strands given by $f(\mu_p), f(\mu_q), f(\mu_r)$ must have the same counterclockwise order as those given by μ_p, μ_q, μ_r. Thus the cyclically ordered addresses $(\mu_p\omega_1, \mu_q\omega_2, \mu_r\omega_3)$ for p will be in the same order as those for $f(p)$, which are $(f(\mu_p\omega_1), f(\mu_q\omega_2), f(\mu_r\omega_3))$. □

Definition 3.1.5. Let T_{BB} be the group of piecewise-linear orientation preserving homeomorphisms $f\colon J(\phi) \to J(\phi)$. △

Proposition 3.1.6. *The set T_{BB} is a group.*

Sketch of proof. The set $\{\mathsf{T}, \mathsf{B}, \mathsf{L}, \mathsf{R}\}^\infty$ is homeomorphic to a Cantor set. The set of piecewise-linear bijections on $\{\mathsf{T}, \mathsf{B}, \mathsf{L}, \mathsf{R}\}^\infty$ form a group similar to Thompson's group V. In particular, it is the group $G_{4,3}$ in [6]. Thus T_{BB} descends from a subgroup of $G_{4,3}$. □

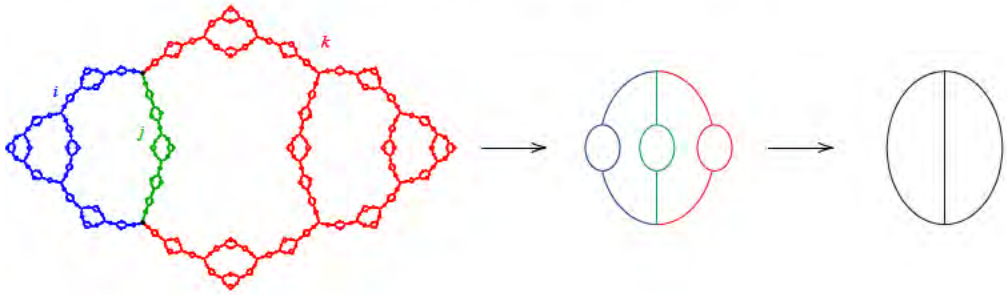

Figure 3.2.1: We reduce the Bubble Bath to its most basic bubble diagram.

3.2 Bubble Diagrams

Before we begin to explore the properties of T_{BB} we want to develop some graphical tools for dealing with its elements. The geometric address system gives us a very easy way to draw simplistic versions of the Bubble Bath. We will pair two of these drawings to represent an $f \in T_{BB}$.

A **bubble diagram** is a drawing of the Bubble Bath Julia set that includes a minimal amount of information. Each bubble diagram includes at least three lines representing the three main strands i, j, and k. Every line in a bubble diagram represents a basic strand. The intersection of three lines represents a triple point. Figure 3.2.1 shows how we reduce the Bubble Bath to its most basic bubble diagram.

Suppose we want to draw a basic strand $\mu\mathsf{X}$ where $\mathsf{X} \in \{\mathsf{T}, \mathsf{B}, \mathsf{L}, \mathsf{R}\}$. Then we first draw

1. the three strands $\mu\mathsf{Y}$ with $\mathsf{Y} \in \{\mathsf{T}, \mathsf{B}, \mathsf{L}, \mathsf{R}\} - \{\mathsf{X}\}$

2. each strands required for drawing μ

These rules define a recursive process which continues until we reach the main strands, which we have already drawn.

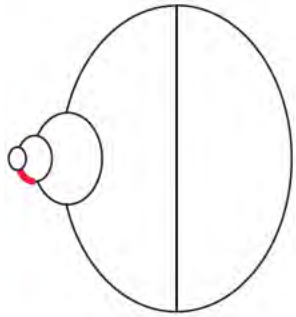

Figure 3.2.2: The strand highlighted in red has address $i\mathsf{LLB}$.

Example 3.2.1. Figure 3.2.2 shows a bubble diagram with the $i\mathsf{LLB}$ strand labeled. Notice how we had to draw in the $i\mathsf{LLT}, i\mathsf{LLL}, i\mathsf{LLR}$ as well as four other strands with length 3 and another four with length 2. ◊

Definition 3.2.2. Let $f \in T_{BB}$. The **bubble diagram pair** for f is an ordered pair of bubble diagrams. Let $\{\mu_i\}_{i=1}^n$ and $\{\lambda_i\}_{n=1}^n$ give the topological partitions in the domain and range of f. In the first bubble diagram, draw a line in a unique color for each μ_i and adorn it with an arrow pointing towards the top triple point of μ_i. To draw the second bubble diagram, draw a line for each λ_i with a coloring such that each $f(\mu_i)$ is the same color as μ_i. Adorn each line in the second diagram with an arrow according to the orientation of the corresponding λ_i – the arrow should point towards the bottom triple point when $f(\mu\omega) = \lambda\omega^*$. See Figure 3.2.3 (a). △

In fact, this definition is overkill. All we really need is a single arrow in each of the domain and the range. Let μ be the strand with the arrow in the domain. Then we'll place the arrow in the range on $f(\mu)$. Since f is bijective, every strand in the domain will be represented in the range. Since f is continuous and orientation preserving, the single arrow will determine where to draw the rest of the strands in the range. See Figure 3.2.3 (b). The function represented in this figure is quite important, so we give it a name.

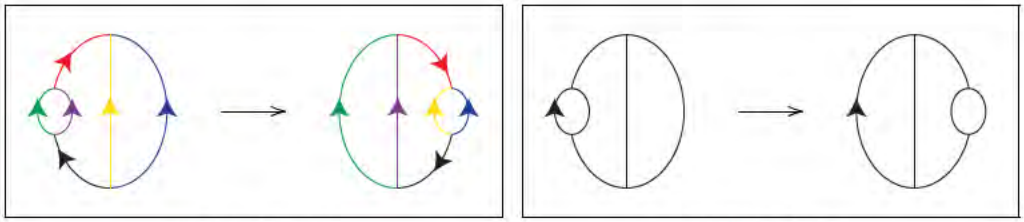

(a) Overlabelled (b) Much better

Figure 3.2.3: Two bubble diagram pairs for the function α.

Definition 3.2.3. Let $\alpha\colon J(\phi) \longrightarrow J(\phi)$ be defined in terms of geometric addresses by

$$\begin{array}{lll} \alpha(i\mathsf{L}\omega) = i\omega & \alpha(j\omega) = k\mathsf{L}\omega & \alpha(k\omega) = k\mathsf{R}\omega \\ \alpha(i\mathsf{R}\omega) = j\omega & & \\ \alpha(i\mathsf{T}\omega) = k\mathsf{T}\omega^* & & \\ \alpha(i\mathsf{B}\omega) = k\mathsf{B}\omega^* & & \end{array}$$

for any $\omega \in \{\mathsf{T}, \mathsf{B}, \mathsf{L}, \mathsf{R}\}^\infty$. Geometrically, α expands the largest bubble on the i strand so that it takes up both the i and k strands. It pushes everything else into the k strand to make room. △

Example 3.2.4 (Proof that $\alpha \in T_{BB}$)**.** The topological partitions are

$$\{i\mathsf{L}, i\mathsf{R}, i\mathsf{T}, i\mathsf{B}, j, k\} \quad \text{and} \quad \{i, j, k\mathsf{T}, k\mathsf{B}, k\mathsf{L}, k\mathsf{R}\}.$$

The equalities guarantee piecewise-linearity. Since each strand only appears once, α is bijective. There are four triple points to check. First, there are π_1 and π_2. Since

$$\alpha(i\overline{\mathsf{T}}) = i\mathsf{T}\overline{\mathsf{B}}, \quad \alpha(j\overline{\mathsf{T}}) = k\mathsf{L}\overline{\mathsf{T}}, \quad \text{and} \quad \alpha(k\overline{\mathsf{T}}) = k\mathsf{R}\overline{\mathsf{T}},$$

we see that α is orientation preserving at π_1. Since

$$\alpha(k\overline{\mathsf{B}}) = k\mathsf{R}\overline{\mathsf{B}} \quad \alpha(j\overline{\mathsf{B}}) = k\mathsf{L}\overline{\mathsf{B}}, \quad \text{and} \quad \alpha(i\overline{\mathsf{B}}) = i\mathsf{B}\overline{\mathsf{T}},$$

we see that α is orientation preserving at π_2. The other two triple points are a partner pair and have addresses $i\mathsf{T}\overline{\mathsf{B}}, i\mathsf{L}\overline{\mathsf{T}}, i\mathsf{R}\overline{\mathsf{T}}$ and $i\mathsf{B}\overline{\mathsf{T}}, i\mathsf{R}\overline{\mathsf{B}}, i\mathsf{L}\overline{\mathsf{B}}$ respectively in the standard cyclic order. We note that

$$\alpha(i\mathsf{T}\overline{\mathsf{B}}) = k\overline{\mathsf{T}}, \quad \alpha(i\mathsf{L}\overline{\mathsf{T}}) = i\overline{\mathsf{T}}, \quad \alpha(i\mathsf{R}\overline{\mathsf{T}}) = j\overline{\mathsf{T}}$$

and that

$$\alpha(i\mathsf{B}\overline{\mathsf{T}}) = k\overline{\mathsf{B}}, \quad \alpha(i\mathsf{R}\overline{\mathsf{B}}) = j\overline{\mathsf{B}}, \quad \alpha(i\mathsf{L}\overline{\mathsf{B}}) = i\overline{\mathsf{B}}. \qquad \Diamond$$

The reader should check that the bubble diagram pair for α is indeed given by Figure 3.2.3 (b). Here is another function we find particularly useful.

Definition 3.2.5. Let γ be defined by

$$\gamma(i\omega) = j\omega \qquad \gamma(j\omega) = k\omega \qquad \gamma(k\omega) = i\omega.$$

for any $\omega \in \{\mathsf{T}, \mathsf{B}, \mathsf{L}, \mathsf{R}\}^\infty$. We can see that γ is simply a three-cycle that permutes the three main strands. The bubble diagram pair for γ is

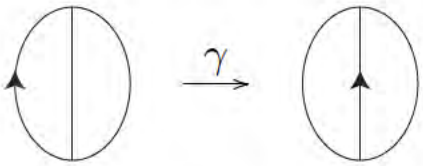

$\triangle$

Since these are group elements, we should have a way to combine their bubble diagrams. We will show to do this by another example.

Example 3.2.6 (Composing Bubble Diagram Pairs)**.** Consider the bubble diagram pairs above for α and γ. The steps to construct the bubble diagram pair for $\alpha \circ \gamma$ are as follows.

1. Position the two diagrams pairs next to each other. Compare the codomain of γ to the domain of α. Here we note that α is more complicated.

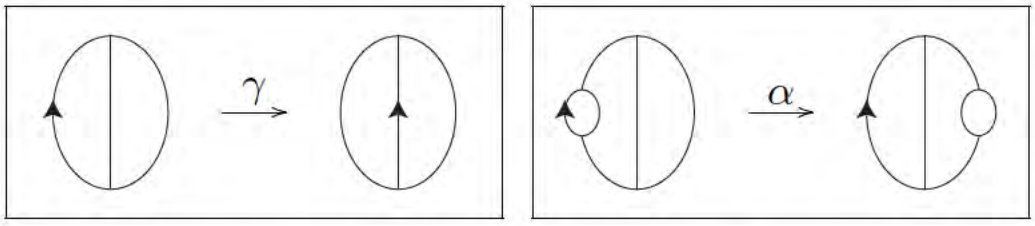

2. Expand the bubble diagram for the codomain of γ so that it matches the domain of α. In general, we may need to expand both to make them match. Choose any new

arrow assignment.

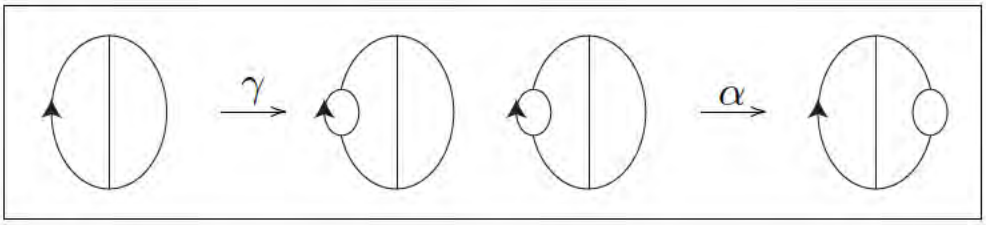

3. Pull back the new bubble diagram we have in the place of the codomain of γ. Remember to pull back the arrow as well. Push forward the new bubble diagram in the place of the domain of α (here this does nothing since we did not change it).

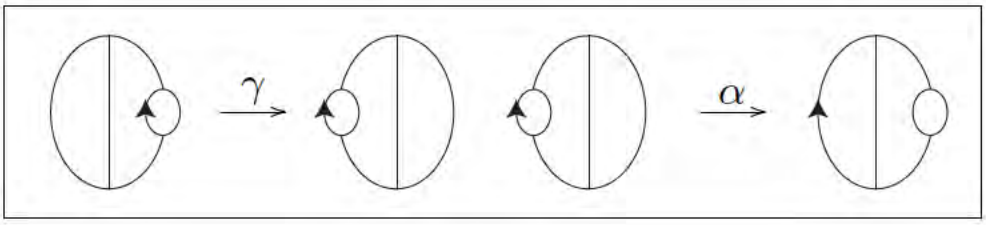

4. Eliminate the extraneous middle diagrams.

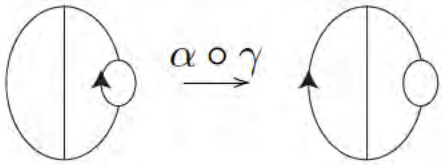

5. Reduce. Here there is nothing to reduce, see the next example.

◊

We should also have inverses, but these are simply the same diagrams in reverse.

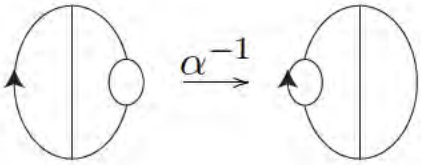

Example 3.2.7 (Inverses and **Reducing**). Suppose we want to construct a bubble diagram pair for $\alpha^{-1}\alpha$. Obviously, this should be the diagram for the identity e

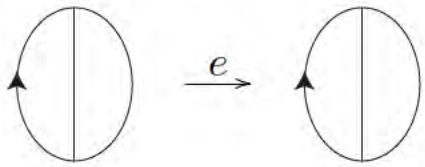

But after following our process, we end up with

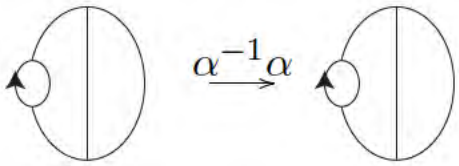

But we can clearly see that nothing has moved on the entire i strand. This means that drawing in the strands $i\mathsf{L}, i\mathsf{R}, i\mathsf{T}, i\mathsf{B}$ is unnecessary. **Reducing** is the process of recognizing unnecessary strand topological partitions and replacing them with the larger "super-strand". In this case, we replace the above strands with i. This gives us the identity bubble diagram pair. ◊

Now that we have introduced the concept of reducing, we can assert the following.

Proposition 3.2.8. *Every element of T_{BB} has a unique reduced bubble diagram pair.*

Rather than offering proof we point the reader to Proposition 5.2 in [4]. The argument is the same, but we insert "basic strand" for "standard interval" and make a few minor adjustments. Furthermore, the reader should not find this proposition surprising in the least because the function f_{geom} from which f descends is defined on basic strands which are exactly what we draw when drawing a bubble diagram.

Definition 3.2.9. Let $f \in T_{BB}$. Then the **complexity** of f is the number of strands in the reduced bubble diagram pair for f. △

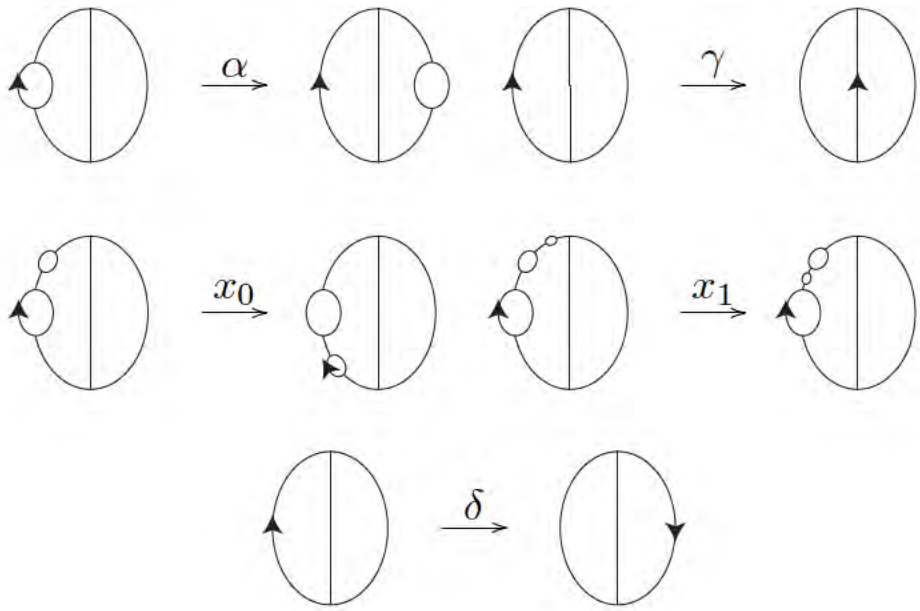

Figure 3.2.4: Bubble diagram pairs for five generators of T_{BB}.

Example 3.2.10. Figure 3.2.4 gives five examples by drawing the diagram pairs for the functions defined at the beginning of Section 3.2.4 defined below. In order, they have complexity 6, 3, 9, 12, and 3. ◊

3.3 Generators

We will skip the proofs that each of the functions given in this section truly is an element of T_{BB} because they are fairly mechanical, and all resemble the one for α in Example 3.2.4. In the next section we will prove that, together with α and γ from Section 3.2, they generate all of T_{BB}.

Definition 3.3.1. Let δ be a 180° rotation around the largest bubble on the j strand so that the π_1 and π_2 switch places. Symbolically,

$$\delta(i\omega) = k\overline{\omega} \qquad \delta(j\omega) = j\overline{\omega} \qquad \delta(k\omega) = i\overline{\omega}. \qquad \triangle$$

In fact, δ sends *every* top triple point to a bottom triple point and every bottom triple point to a top triple point. It is the ultimate flip.

Definition 3.3.2. Let x_0 be defined by

$$\begin{aligned} x_0(i\mathsf{TT}\omega) &= i\mathsf{T}\omega \\ x_0(i\mathsf{TL}\omega) &= i\mathsf{L}\omega \\ x_0(i\mathsf{TR}\omega) &= i\mathsf{R}\omega \\ x_0(i\mathsf{TB}\omega) &= i\mathsf{BT}\omega \\ x_0(i\mathsf{L}\omega) &= i\mathsf{BL}\omega \\ x_0(i\mathsf{R}\omega) &= i\mathsf{BR}\omega \\ x_0(i\mathsf{B}\omega) &= i\mathsf{BB}\omega \end{aligned} \qquad x_0(j\omega) = j\omega \qquad x_0(k\omega) = k\omega$$

for all $\omega \in \{\mathsf{T}, \mathsf{B}, \mathsf{L}, \mathsf{R}\}^\infty$. △

Definition 3.3.3. Let x_1 be defined by

$$\begin{aligned} x_0(i\mathsf{TTT}\omega) &= i\mathsf{TT}\omega \\ x_0(i\mathsf{TTL}\omega) &= i\mathsf{TL}\omega \\ x_0(i\mathsf{TTR}\omega) &= i\mathsf{TR}\omega \\ x_0(i\mathsf{TTB}\omega) &= i\mathsf{TBT}\omega \\ x_0(i\mathsf{TL}\omega) &= i\mathsf{TBL}\omega \\ x_0(i\mathsf{TR}\omega) &= i\mathsf{TBR}\omega \\ x_0(i\mathsf{TB}\omega) &= i\mathsf{TBB}\omega \\ x_0(i\mathsf{L}\omega) &= i\mathsf{L}\omega \\ x_0(i\mathsf{R}\omega) &= i\mathsf{R}\omega \\ x_0(i\mathsf{B}\omega) &= i\mathsf{B}\omega \end{aligned} \qquad x_0(j\omega) = j\omega \qquad x_0(k\omega) = k\omega$$

for all $\omega \in \{\mathsf{T}, \mathsf{B}, \mathsf{L}, \mathsf{R}\}^\infty$. △

It is not hard to see from Figure 3.2.4 that x_0 and x_1 are quite similar to two of the generators of Thompson's group T from Section 1.5. We simply identify the bubble between the j and k strands with the point 0 and identify each bubble on the i strand with a dyadic rational on the circle. Figure 3.3.1 shows a clarifying example. This labeling is equivalent to using the dyadic rational subset of the internal angles from Section 2.1.

Consider the composition $\delta\alpha$ given by the bubble diagram pair

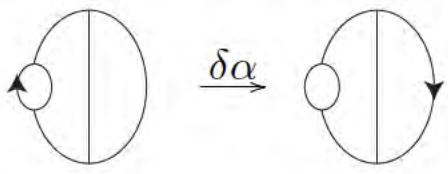

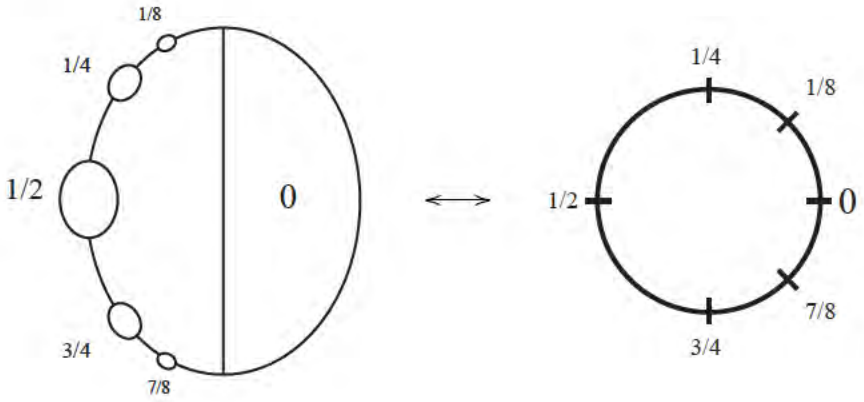

Figure 3.3.1: Some elements of T_{BB} are identified with elements of Thompson's group T. This labeling is equivalent to the internal angles from Section 2.1.

This element $\delta\alpha$ is the third generator for our copy of T.

Theorem 3.3.4. *The group generated by $\langle x_0, x_1, \delta\alpha\rangle$ is isomorphic to Thompson's group T.*

Figure 3.3.1 is as good as any proof.

Corollary 3.3.5. *The group generated by $\langle x_0, x_1\rangle$ is isomorphic to Thompson's group F.*

These results lend us enormous power the over the i strand. In particular, let S and Q be finite sets of n bubbles that are either the middle bubble or are on the i strand. Then we can move the bubbles in S to the bubbles in Q as long as we preserve their cyclic order.

3.4 Proof of Generation

In this section we will prove that T_{BB} is generated by a set of four generators. However, this result follows immediately if it is generated by five. Thus the central focus of this section will be to prove the following:

Theorem 3.4.1. *T_{BB} is generated by $\{x_0, x_1, \alpha, \delta, \gamma\}$.*

Lemma 3.4.2. *Each of the generators $\{x_0, x_1, \alpha, \delta, \gamma\}$ is contained in the group T_{BB}.*

Proof. Clearly, each generator descends from a piecewise-linear bijection. We simply need to check for continuity at triple points and that they are all orientation preserving. The reader can use Example 3.2.4 as a model and fill in the details. □

Lemma 3.4.3. *The group $\langle x_0, x_1, \alpha, \delta, \gamma \rangle$ acts transitively on triple points of the Bubble Bath Julia set.*

Proof. Let $p \in J(\phi)$ be a triple point. We will show that we can map p to π_1 using only the generators given in the hypothesis. If $p = \pi_1$, we're done. If $p = \pi_2$, we apply δ and we're done. If p is a bottom fixed point, we apply δ so that it becomes a top triple point. So we can suppose that p is a top triple point other than π_1.

We know p has three addresses. Since all the generators are continuous, we can simply choose one address. We choose $\mu\mathsf{L}\overline{\mathsf{T}}$ for the appropriate finite address μ. We will use the generators to reduce this address to $i\overline{\mathsf{T}}$, the address for π_1. Let μ have n letters. We proceed by induction on n.

Base Case: We know that $n \neq 0$ because μ must include an i, j, or k. If $n = 1$, then we have three cases. If $\mu = i$, we simply apply α and have $\alpha(i\mathsf{L}\overline{\mathsf{T}}) = i\overline{\mathsf{T}}$ and we are done. If $\mu = j$ or k, we apply γ or γ^2 respectively. This puts us in the case where $\mu = i$.

Inductive Step: Now we will use cases to show that for any n, we can use our generators to reduce the number of letters in μ to $n - 1$.

1. Let $\mu = j\mu'$ or $k\mu'$. Apply γ or γ^2 (respectively) so that j or k becomes i. Now we are in one of the following three cases.

2. Let $\mu = i\mathsf{L}\mu'$. Apply α, now we have $\alpha(i\mathsf{L}\mu') = i\mu'$ with length $n - 1$.

3. Let $\mu = i\mathsf{R}\mu'$. Apply α, now we have $\alpha(i\mathsf{R}\mu') = j\mu'$.

4. Let $\mu = i\mathsf{T}\mu'$ or $i\mathsf{B}\mu'$. Recall that we have all the power of Thompson's group T. Thus we can apply the appropriate combination of x_0 and x_1 to move the bubble that our triple point sits on the bubble at angle $\frac{1}{2}$. This both reduces the length of μ and puts us in one of the last two cases. Rigorously, we need to break it into more cases. Note that

$$x_0(i\mathsf{TR}\mu') = i\mathsf{R}\mu' \qquad x_1^{-1}(i\mathsf{TBR}\mu') = i\mathsf{TR}\mu'$$
$$x_0(i\mathsf{TL}\mu') = i\mathsf{L}\mu' \qquad x_1^{-1}(i\mathsf{TBL}\mu') = i\mathsf{TL}\mu'$$
$$x_0(i\mathsf{TT}\mu') = i\mathsf{T}\mu' \qquad x_1^{-1}(i\mathsf{TBB}\mu') = i\mathsf{TB}\mu'$$
$$x_0x_1^{-1}(i\mathsf{TBT}\mu') = x_0(i\mathsf{TTB}\mu') = i\mathsf{TB}\mu'$$

□

Lemma 3.4.4. *Let $f \in T_{BB}$. If f fixes π_1 or π_2, then f fixes the other one.*

The two fixed points π_1 and π_2 are uniquely paired from a topological perspective but the argument includes some topological assumptions about $J(\phi)$ which we are not prepared to prove. We already know that $J(\phi)$ is compact and Hausdorff, and path connected (theorems from [13]) but the following argument assumes some things about *how* $J(\phi)$ it is path connected. In particular, it seems clear from the picture that for any triple point, there is a unique second triple point such that if you remove both you will have disconnected the Julia set into three pieces. However, this is "from the picture". To make this proof rigorous, it would take some further investigation into [13] and probably some other sources.

Proof. Without loss of generality, suppose that f fixes the top fixed point π_1.

Consider the set $S = J(\phi) - \{\pi_1\}$. The point π_2 is the unique point such that $S - \{\pi_2\}$ is disconnected into three connected components. Since $f(\pi_1) = \pi_1$, we see that $f(S) = S$, so π_2 is also the unique point that disconnects $f(S)$.

Since f is a homeomorphism, it maps connected components to connected components. So $f(J(\phi) - \{\pi_1, \pi_2\}) = J(\phi) - \{\pi_1, \pi_2\}$. Thus $f(\{\pi_1, \pi_2\}) = \{\pi_1, \pi_2\}$. Since $f(\pi_1) = \pi_1$ and is bijective, $f(\pi_2) = \pi_2$. □

This Lemma generalizes with the same argument to prove that indeed every triple point is uniquely paired with its partner pair from Definition 2.2.4. Furthermore, combining Lemmas 3.4.3 and 3.4.4 gives the following corollary.

Corollary 3.4.5. *The group $\langle x_0, x_1, \alpha, \delta, \gamma \rangle$ acts transitively on triple point partner pairs of the Bubble Bath Julia set.*

Armed with this we can finish our proof.

Proof of Theorem 3.4.1. Let $f \in T_{BB}$. We use induction on the complexity (from Definition 3.2.9) of the bubble diagram pair of f. To this end, we will color every basic strand in our bubble diagram pairs with either black or red. The black strands are strands where f is the identity. A strand S is red when some part of it is in the support of f. In other words, when we have left out some of the substrands of S that we would normally draw. Red strands will always be sent to red strands, and thus omit the same number of strands in each of the domain and codomain. This guarantees that complexity is still well defined. See Figure 3.4.1.

The base case is obvious. All we must show is that for f with complexity n, we can apply our generators to f to make an element with complexity less than n.

By our two lemmas we may assume that the two fixed points are fixed by f. Since f is a homeomorphism, it must map each of the main strands to another main strand and preserve their counterclockwise order. Using γ, we can suppose that each main strand maps to itself. Thus we can write $f = f_i f_j f_k$ where f_i acts solely on the i strand and similarly with f_j and f_k as in Figure 3.4.1. If more than one of these is non-trivial, then each of their bubble diagram pairs must have complexity less than n and our induction is

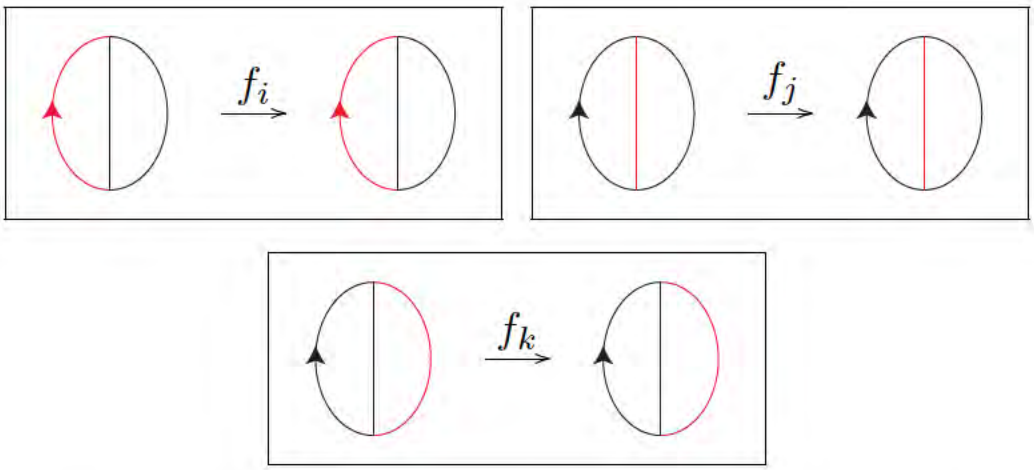

Figure 3.4.1: We can split an arbitrary $f \in T_{BB}$ into a product $f_i f_j f_k$.

finished. Conjugating by a power of γ, we may suppose without loss of generality that f_i is the non-trivial one.

Now, by using the power of Thompson's group F, we can apply combinations of our elements x_0 and x_1 in such a way that we may assume that the two triple points of the main bubble on the i strand are fixed. Since f is continuous, it must map each of the four strands $\mathsf{T}, \mathsf{B}, \mathsf{L}$, and R to themselves. By the same argument as above, we can suppose that only one of $f_{\mathsf{T}}, f_{\mathsf{B}}, f_{\mathsf{R}}$, and f_{L} is non-trivial. We address these in cases.

1. Suppose f_{L} is non-trivial. The function $\alpha f \alpha^{-1}$ is simpler than f. See Figure 3.4.2 (a).

2. Suppose f_{R} is non-trivial. The function $\alpha\gamma^2 f \gamma^{-2}\alpha^{-1}$ is simpler than f. The picture is nearly the same in case 1.

3. Suppose f_{T} is non-trivial. Since their are finitely many breakpoints, there are finitely many bubbles in T for which f_{T} is not the identity. Let X be the set of such bubbles. Let $B \in X$ be the bubble with greatest the internal angle as according to Defini-

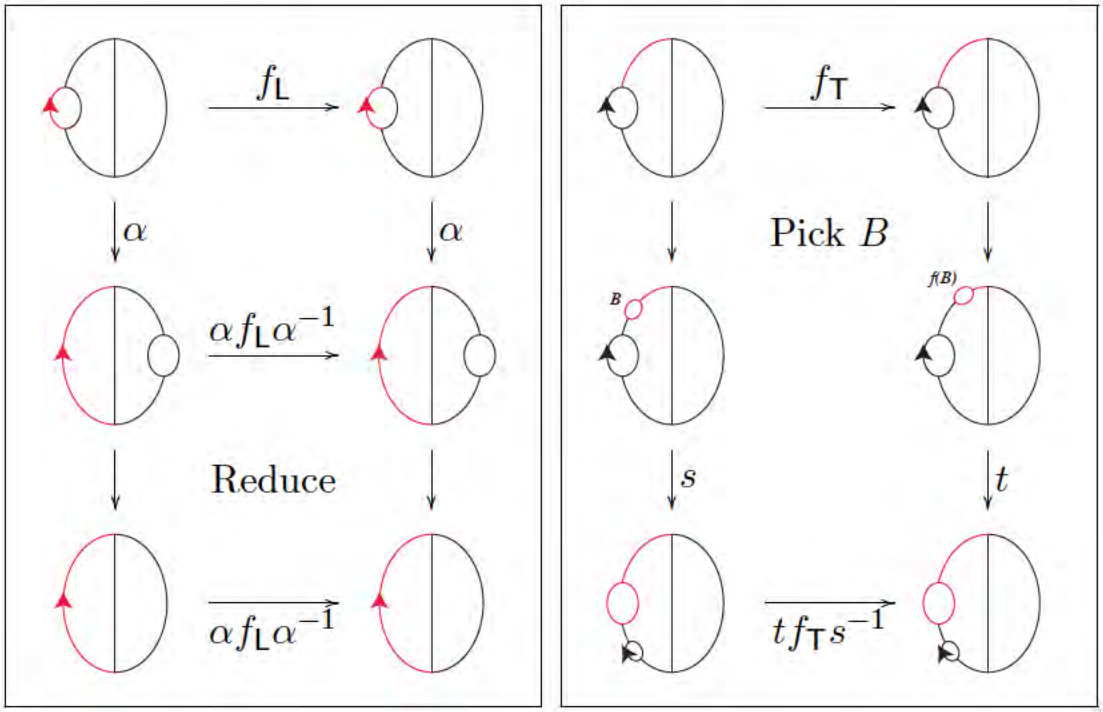

(a) The function $\alpha f_L \alpha^{-1}$ is simpler than f_L.

(b) The bubble diagram pair for $t f_T s^{-1}$ is reducible.

Figure 3.4.2: We apply generators to reduce the complexity of various $f \in T_{BB}$.

tion 2.1.3 and Figure 3.3.1. Using our copy of Thompson's group F, there exists elements $s, t \in \langle x_0, x_1 \rangle$ such that

(a) the bubble diagram pairs for both s and t have the same complexity

(b) s sends B to the $\frac{1}{2}$-bubble and t sends $f_T(B)$ to the $\frac{1}{2}$-bubble

(c) both send the $\frac{1}{2}$-bubble to the the $\frac{3}{4}$-bubble

Now the element tfs^{-1} is simpler than f. See Figure 3.4.2 (b).

4. Suppose f_B is non-trivial. This case is similar to 3.

□

Corollary 3.4.6. *The sets*

$$\langle x_0, x_1, \gamma, \alpha \rangle \qquad \textit{and} \qquad \langle x_0, x_1, \delta\alpha, \gamma, \delta \rangle$$

also generate T_{BB}*.*

Proof. The first one is a consequence of the relation $\delta = (x_0^{-1}\gamma\alpha)x_0(x_0^{-1}\gamma\alpha)^{-1}$. We leave it to the reader to verify this by composing bubble diagram pairs.

The second is obvious, but it is worth mentioning because it clearly displays the copy of T generated by $\langle x_0, x_1, \delta\alpha \rangle$. In Section 3.5 we will mostly use this generating set. □

3.5 Properties of the Group T_{BB}

We are almost ready to investigate the subgroup structure of T_{BB}. We will find that T_{BB} has an index-six simple group that is generated by copies of T. First, however, we will review some useful group theory material. The first few items are from [10],

Definition 3.5.1. Let G be a group acting on a set S. Fix $s \in S$. The **stabilizer** of s is the set

$$G_s = \{g \in G \mid g(s) = s\}. \qquad \triangle$$

It is also true that $G_s \leq G$.

Definition 3.5.2. Let G be a group and let $x, y \in G$. The **commutator** of x and y is $[x, y] = x^{-1}y^{-1}xy$. The **commutator subgroup** of G is

$$[G, G] = \langle \{[x, y] \mid x, y \in G\} \rangle. \qquad \triangle$$

Proposition 3.5.3. *Let G be a group and let $N \leq G$. Then $N \trianglelefteq G$ if and only if $[N, G] \leq N$. In particular, $[G, G] \trianglelefteq G$.*

Proof. Simply note that $g^{-1}ng \in N$ for all $n \in N$ and $g \in G$ if and only if $n^{-1}g^{-1}ng \in N$ for all $n \in N$ and $g \in G$. □

This also implies that if $n \in N \trianglelefteq G$ then $[n, g]$ and $[g, n]$ are in N for all $g \in G$.

Proposition 3.5.4. *Let G be a group, let $H \leq G$, and let $N \trianglelefteq G$. Then $H \cap N \trianglelefteq H$.*

Proof. Because $N \trianglelefteq G$ we know that for all $n \in N$ and $g \in G$, we have $g^{-1}ng \in N$. Let $x \in H \cap N$. Then clearly $h^{-1}xh \in H$ for all $h \in H \cap N$ because N is closed. But since $H \leq G$, we also have $h^{-1}nh \in N$. Thus $h^{-1}xh \in H \cap N$ for all $h \in H$ and so $H \cap N \trianglelefteq H$. □

Definition 3.5.5. Let S be a finite set. Let $G = \langle x_0, x_1, \ldots x_n \rangle$ be a finitely generated group that acts on S. The **Schreier graph** for G acting on S is the directed graph Γ with a vertex for each $s \in S$ and a directed edge $s \longrightarrow x_i(s)$ for each x_i at each vertex. △

Theorem 3.5.6 (Schreier's Lemma)**.** *Let S be a finite set, let G be a finitely generated group that acts on S, and let Γ be the Schreier graph for G acting on S. Let fix $s_0 \in S$. For each $s \in S$, let $g_s \in G$ so that $g_s(s_0) = s$. Then G_{s_0} has one generator for each edge $s \longrightarrow x_i(s)$. This generator is $g^{-1}_{x_i(s)} x_i g_s$.*

Each generator comes from tracing out a loop through the Schreier graph. Starting from s_0, the loop traverses edges until it gets to s. It picks up a generator for each edge so that when it gets to s, it has picked up g_s. Then it picks up x_i as it moves across $s \longrightarrow x_i(s)$. Finally, it picks up $g^{-1}_{x_i(s)}$ as it returns to s_0. Thus, we can find a generating set by carefully tracing out certain loops with base point s_0. For more on Schreier's Lemma, see Theorem 1.12 in [8].

Now we will spend some time developing the set that we want T_{BB} to act on. Consider the three-coloring of the complement of the Bubble Bath shown in Figure 3.5.1. The coloring is rigorously defined on each bubble by the dynamics of ϕ. The orbit of every point in the complement of the Bubble Bath eventually converges to the three cycle $\{0, \infty, -1\}$. Thus, the orbit under $\phi^{\circ 3}$ of every point converges to exactly *one* of these three points.

Figure 3.5.1: A three-coloring of the complement of the Bubble Bath.

Thus for every p in the complement of the Bubble Bath, we color p blue if its orbit under $\phi^{\circ 3}$ converges to 0, green if its orbit converges to ∞, and red if its orbit converges to -1. In other words, the colors are the basins of attraction for the three fixed points of $\phi^{\circ 3}$.

This construction also allows us to simplify the coloring down to a coloring of the three bubbles containing $-1, 0$, and ∞, which we call the **post-critical bubbles**. See Figure 3.5.2. Thus, this coloring, which at first seemed quite complicated, is now reduced to the ordered triple (r, b, g).

The elements of T_{BB} permute the colors in this three-coloring. Because $f \in T_{BB}$ is a homeomorphism, it's enough to understand how f permutes the colored dots on the right of figure Figure 3.5.2. We assert the following, and allow the reader to check.

Lemma 3.5.7. *The group T_{BB} acts on the set of ordered triples with distinct entries in $\{r, b, g\}$ as follows:*

- *$x_0, x_1, \delta\alpha$ all fix the order of the colors.*
- *δ switches the first two colors and leaves the third fixed.*

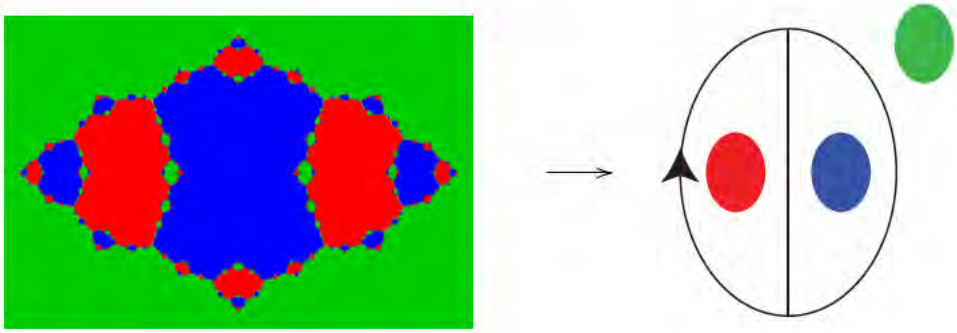

Figure 3.5.2: We can simplify the three-coloring to a simple ordered triple of colors (r, b, g).

- γ *cyclically permutes the order of the colors.*

We let $S_3 = \langle \delta, \gamma \rangle$ be the group of all permutations of the ordered triple (r, b, g). (Please excuse this abuse of the standard notation, as it is trivially isomorphic to the usual S_3.) Now there is a homomorphism $\rho \colon T_{BB} \longrightarrow S_3$. By K we denote the kernel of ρ.

Corollary 3.5.8. *Our group is a semi-direct product $T_{BB} = K \rtimes S_3$. The subgroup K has index six in T_{BB}.*

Proof. This is immediate from the construction of our homomorphism ρ. □

Theorem 3.5.9. *K is generated by six isomorphic copies of T.*

Proof. Let ρ be the homomorphism defined above by the action in Lemma 3.5.7 of T_{BB} on set of ordered triples with distinct entries from $\{r, b, g\}$. Note that the stabilizer of our original coloring $G_{(r,b,g)} = K$.

We construct a Schreier graph for T_{BB} with this action. For the purposes of this proof, we use the generating set $\langle x_0, x_1, \delta\alpha, \gamma, \delta \rangle$ from Corollary 3.4.6. See Figure 3.5.3 for a representation of the associated Schreier graph. For the sake of clarity, the graph is missing an edge for each of $x_0, x_1, \delta\alpha$ at each vertex. Each of these edges is just a loop back to its starting vertex.

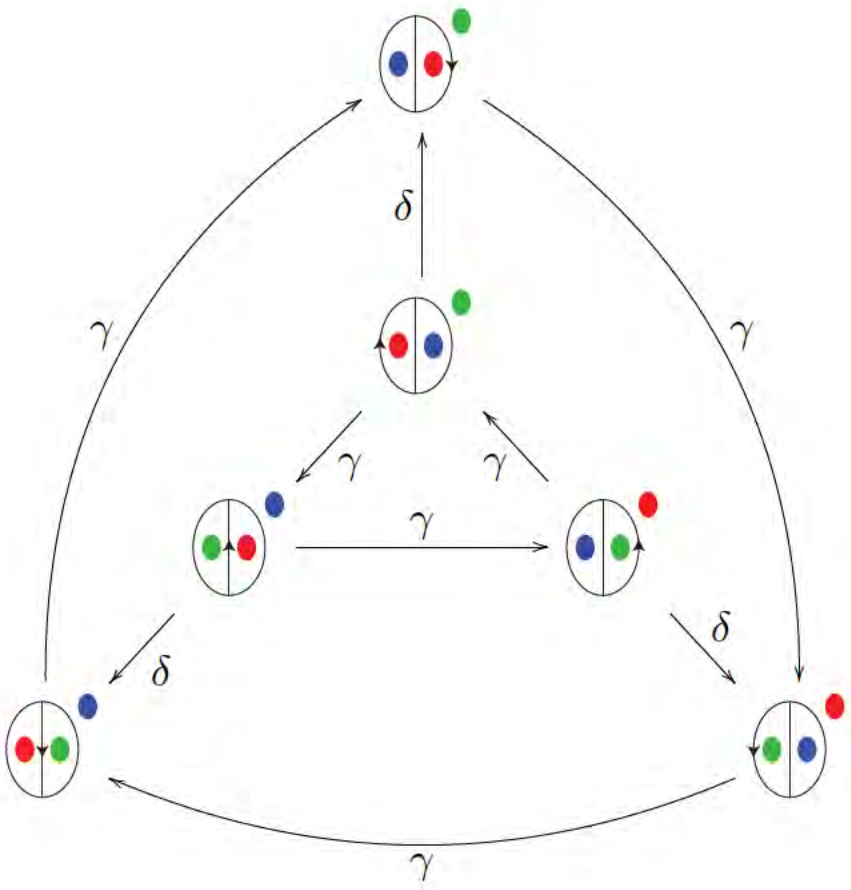

Figure 3.5.3: Schreier graph showing the action of T_{BB} on a coloring of the Bubble Bath. The other generators x_0, x_1, and $\delta\alpha$ fix the colors.

After carefully tracing out many loops, the stabilizer of the original coloring (r, b, g) is generated by

$$\begin{aligned} G_{(r,b,g)} =& \langle x_0, x_1, \delta\alpha, \\ & \gamma x_0 \gamma^{-1}, \gamma x_1 \gamma^{-1}, \gamma(\delta\alpha)\gamma^{-1}, \\ & \gamma^2 x_0 \gamma^{-2}, \gamma^2 x_1 \gamma^{-2}, \gamma^2(\delta\alpha)\gamma^{-2}, \\ & \delta x_0 \delta^{-1}, \delta x_1 \delta^{-1}, \delta(\delta\alpha)\delta^{-1}, \\ & (\delta\gamma^2) x_0 (\delta\gamma^2)^{-1}, (\delta\gamma^2) x_1 (\delta\gamma^2)^{-1}, (\delta\gamma^2)(\delta\alpha)(\delta\gamma^2)^{-1}, \\ & (\delta\gamma) x_0 (\delta\gamma)^{-1}, (\delta\gamma) x_1 (\delta\gamma)^{-1}, (\delta\gamma)(\delta\alpha)(\delta\gamma)^{-1} \rangle. \end{aligned}$$

This is simply six copies of T. Recall from Theorem 3.3.4 that $\langle x_0, x_1, \delta\alpha \rangle \cong T$. The others are simply this generating set conjugated by elements of S_3. □

For each copy of T one of the post-critical bubbles is identified with the point 0 on the unit circle. Similarly, one of the post critical bubbles is identified as the inside of the unit circle, and the last is identified as the outside. We call the original copy of T from Theorem 3.3.4 $T^{\text{Id.}} = \langle x_0, x_1, \delta\alpha \rangle$. For $T^{\text{Id.}}$, the post-critical bubbles are identified as follows: the outside bubble containing ∞ is identified with the outside of the unit circle, the left bubble containing -1 is identified with the inside of the unit circle, and the middle bubble containing zero is identified with the point 0 on the unit circle. Thus, the copy of F contained in $T^{\text{Id.}}$ is generated by $\langle x_0, x_1 \rangle$ and acts on the i strand.

By examining Figure 3.5.3, we can see how each copy of T acts on the Bubble Bath. The original coloring of the Bubble Bath appears second from the top in Figure 3.5.3. It represents $T^{\text{Id.}}$ and has the left bubble red, the middle bubble blue, and the outside bubble green.

Proposition 3.5.10. *Each colored bubble diagram in Figure 3.5.3 represents a copy of T where the red bubble is identified as the inside of the unit circle, the green bubble is the*

outside, and the blue bubble is the point 0*. The copy of* F *inside each* T *acts on the main strand marked with an arrow.*

To find T^f *for* $f \in S_3$*, apply to the original coloring (second from the top) by following the appropriate edges.*[1]

Thus

$$T^{\delta\gamma^2} = \langle (\delta\gamma^2)x_0(\delta\gamma^2)^{-1}, (\delta\gamma^2)x_1(\delta\gamma^2)^{-1}, (\delta\gamma^2)(\delta\alpha)(\delta\gamma^2)^{-1} \rangle$$

also treats the middle bubble as the point 0 but identifies the outside bubble containing ∞ as the inside of the unit circle and the left bubble as the outside of the unit circle. The copy of F contained in $T^{\delta\gamma^2}$ also acts on the i strand. We can see that T^{γ} and $T^{\delta\gamma}$ also share a copy of F, this one on the j strand. And finally, T^{γ^2} and T^{δ} share a copy of F acting on the k strand.

Next we will to prove that K is simple. This will be significantly harder, and require a couple of lemmas.

Definition 3.5.11. Let μ and λ be finite addresses. We say that λ is an **initial segment** of μ when there exists some finite sequence $\{\mathsf{X}_i\}_{i=1}^n$ with each $\mathsf{X}_i \in \{\mathsf{T}, \mathsf{B}, \mathsf{L}, \mathsf{R}\}$ such that

$$\mu = \lambda \mathsf{X}_1 \mathsf{X}_2 \dots \mathsf{X}_n. \qquad \triangle$$

Lemma 3.5.12. *Let* μ, λ *be finite addresses for the basic strands* S *and* S' *respectively.*

1. $S \subseteq S'$ *if and only if* λ *is an initial segment of* μ
2. $S' \subseteq S$ *if and only if* μ *is an initial segment of* λ

If neither S *or* S' *is a subset of the other, then* $S \cap S'$ *is the set of common endpoints.*

[1] We should clarify our notation here. Recall that all the generators are indeed functions. When we write them next to each other, the implied "multiplication" is composition, even though we have not included the standard $\circ$. As such, they should be read right to left. Thus, if we want to find the colored bubble diagram showing $T^{\delta\gamma^2}$ in Figure 3.5.3, we should start at the original coloring (second from the top) and follow two edges labeled γ and *then* follow an edge labeled δ. This should take us to the vertex at the bottom right.

Proof.

1. Let λ be an initial segment of μ, and let $p \in S$. In particular, suppose that $\mu = \lambda \mathsf{X}_1\mathsf{X}_2 \dots \mathsf{X}_n$ with each $\mathsf{X}_i \in \{\mathsf{T}, \mathsf{B}, \mathsf{L}, \mathsf{R}\}$. Then p has an address $\mu\omega$ for some $\omega \in \{\mathsf{T}, \mathsf{B}, \mathsf{L}, \mathsf{R}\}^\infty$. But $\mu\omega = \lambda \mathsf{X}_1\mathsf{X}_2 \dots \mathsf{X}_n\omega$ and $\mathsf{X}_1\mathsf{X}_2 \dots \mathsf{X}_n\omega \in \{\mathsf{T}, \mathsf{B}, \mathsf{L}, \mathsf{R}\}^\infty$. So $p \in S'$.

   Conversely, let $S \in S'$. Then $p \in S$ implies $p \in S'$. Thus for all $\omega \in \{\mathsf{T}, \mathsf{B}, \mathsf{L}, \mathsf{R}\}^\infty$ there exists a $\omega_1 \in \{\mathsf{T}, \mathsf{B}, \mathsf{L}, \mathsf{R}\}^\infty$ such that the address of p is $\mu\omega = \lambda\omega_1$. Since it's true for all ω, we conclude that λ must be an initial segment of μ. If it did not, we could choose an ω so that $\mu\omega \neq \lambda\omega_1$ for all ω_1.

2. The proof is quite similar to 1, so we will omit it.

Suppose that neither is a subset of the other and let $p \in S \cap S'$. Then p has two addresses. The only points with multiple itineraries are triple points, so the only points with multiple addresses are triple points. If p is not an endpoint of S and S', then the intersection would include non-triple points because S and S' are connected. □

Lemma 3.5.13. *Let $f \in T_{BB}$ and suppose f is not the identity. Then there exists a basic strand that f maps to a disjoint basic strand.*

Proof. Let f_{geom} be the piecewise-linear bijection that descends to f. Since f is non-trivial, f_{geom} must be non-trivial. Then some basic strand in the domain of f_{geom} is sent to some other basic strand, or every strand is flipped and sent to itself. The latter clearly violates the continuity of f, so there must exist some basic strand S with finite address μ such that $f_{\text{geom}}(\mu\omega) = \lambda\omega$ or $\lambda\omega^*$ for some finite address $\lambda \neq \mu$ and all $\omega \in \{\mathsf{T}, \mathsf{B}, \mathsf{L}, \mathsf{R}\}^\infty$.

Now we apply Lemma 3.5.12 to the basic strands S and $f(S)$. We have three cases.

Case 1: Suppose that neither S nor $f(S)$ is contained in the other. Then $S \cap f(S) \subseteq \{p, q\}$ for triple points p, q at the top and bottom of S respectively. Consider the substrand

$S' \subseteq S$ with finite address $\mu\mathsf{L}$. The endpoints of S are not in S' and $f(S') \subseteq f(S)$ Thus $S' \cap f(S') = \emptyset$.

Case 2: Suppose that $S \subseteq f(S)$. Let $\mu = \lambda \mathsf{X}_1\mathsf{X}_2 \dots \mathsf{X}_n$ for each $\mathsf{X}_i \in \{\mathsf{T}, \mathsf{B}, \mathsf{L}, \mathsf{R}\}$. Let $\mathsf{Y} \in \{\mathsf{T}, \mathsf{B}, \mathsf{L}, \mathsf{R}\} - \{\mathsf{X}_1, \mathsf{X}_1^*\}$ and let $S' \subseteq S$ be the basic strand with finite address $\mu\mathsf{Y}$. Now we have two basic strands S' and $f(S')$ with finite addresses $\mu\mathsf{Y} = \lambda\mathsf{X}_1\mathsf{X}_2 \dots \mathsf{X}_n\mathsf{Y}$ and $\lambda\mathsf{Y}$ or $\lambda\mathsf{Y}^*$, respectively. Then neither is an initial segment of the other, so now we are in Case 1.

Case 3: Suppose $f(S) \subseteq S$. Let $\lambda = \mu\mathsf{X}_1\mathsf{X}_2 \dots \mathsf{X}_n$ for each $\mathsf{X}_i \in \{\mathsf{T}, \mathsf{B}, \mathsf{L}, \mathsf{R}\}$. Let $\mathsf{Y} \in \{\mathsf{T}, \mathsf{B}, \mathsf{L}, \mathsf{R}\} - \{\mathsf{X}_1, \mathsf{X}_1^*\}$ and let $f(S)' \subseteq f(S)$ be the basic strand with finite address $\lambda\mathsf{Y}$. Now we have a substrand $S' \subseteq S$ given by the finite address $\mu\mathsf{Y}$ or $\mu\mathsf{Y}^*$. We compare the finite addresses of S' and $f(S')$ and see that neither is an initial segment of the other. Now we are in Case 1. □

With this lemma we should be able model our proof on the one for Theorem 8.3 in [4]. This will prove that K is simple! First, recall the definition of support.

Definition 3.5.14. The **support** of a function $f \in T_{BB}$ is the set

$$\text{supp}(f) = \{x \in \text{ Bubble Bath} \mid f(x) \neq x\}. \qquad \triangle$$

Proposition 3.5.15. *Let $f, g \in T_{BB}$. Then*

1. $f(\text{supp}(f)) = \text{supp}(f)$.
2. $\text{supp}(f^{-1}) = \text{supp}(f)$.
3. *If* $\text{supp}(f) \cap \text{supp}(g) = \emptyset$, *then* $fg = gf$.
4. $\text{supp}(g^{-1}fg) = g(\text{supp}(f))$.

Theorem 3.5.16. *The kernel K is simple, and every non-trivial normal subgroup of T_{BB} contains K.*

Proof. Let N be a non-trivial normal subgroup of K or of T_{BB}. Note that, in either case, the commutator $[n,k] \in N$ for all $n \in N$ and $k \in K$. We must prove that N contains K.

Let $f \in N$ be non-trivial. By Lemma 3.5.13, there exists a basic strand S such that $S \cap f(S) = \emptyset$. Without loss of generality, we can assume that, in the three-coloring, S has green on its left, and red on its right. (We can always choose a substrand of S with this color combination.)

Since T_{BB} acts transitively on partner pairs of triple points, there exists $y \in T_{BB}$ such that $y(S)$ is one of the main basic strands with address i, j, or k. Since $T_{BB} \cong K \rtimes S_3$, there exists a $\sigma \in \langle \delta, \gamma \rangle \cong S_3$ such that $\sigma y \in K$. Note that σ simply permutes the three main strands. Let $z = \sigma y$. We already know $z(S)$ is one of the three main strands, but since $z \in K$ it preserves the three-coloring, so $z(S)$ will have green on the left, and red on the right. Thus $z(S)$ is the i strand.

Let $g, h \in T_{BB}$ with $\text{supp}(f) \subseteq S$ and $\text{supp}(g) \subseteq S$. Such elements exist because T_{BB} acts transitively on partner pairs of triple points. By Proposition 3.5.15 (4), the conjugate $f^{-1}g^{-1}f$ has support in $f(S)$. Since

$$\text{supp}(h) \cap \text{supp}(f^{-1}g^{-1}f) = \emptyset = \text{supp}(g) \cap \text{supp}(f^{-1}g^{-1}f),$$

we use Proposition 3.5.15 (3) and have

$$\begin{aligned}
\big[[g,f],h\big] =& [g,f]^{-1}h^{-1}[g,f]h \\
=& (g^{-1}f^{-1}gf)^{-1}h^{-1}(g^{-1}f^{-1}gf)h \\
=& (f^{-1}gf)^{-1}gh^{-1}g^{-1}(f^{-1}gf)h \\
=& gh^{-1}g^{-1}h \\
=& [g^{-1},h].
\end{aligned}$$

Since $f \in N$, by Proposition we know 3.5.3 $[g, f] \in N$. So by the same logic $\big[[g, f], h\big] \in N$ also and so $[g^{-1}, h] \in N$. Since $\text{supp}(g) = \text{supp}(g^{-1})$, we have proved that the commutator $[g, h] \in N$ for any $g, h \in T_{BB}$ with support in S.

Now, let $g, h \in T_{BB}$ have support on the i strand. Since $z(S)$ is the i strand, the functions zgz^{-1} and zhz^{-1} both have support on S by Proposition 3.5.15 (4). Thus, the commutator $[zgz^{-1}, zhz^{-1}] = z[g, h]z^{-1} \in N$. But since N is normal in K or in T_{BB}, we know that it is closed under conjugation by $z \in K$. Thus, we have proved that $[g, h] \in N$ for any $g, h \in T_{BB}$ with support on the i strand.

Recall from Corollary 3.3.5 that $\langle x_0, x_1 \rangle \cong F$. Since F is not abelian, there exist $u, v \in \langle x_0, x_1 \rangle$ such that $[u, v]$ is non-trivial. Since u, v have support on the i strand, $[u, v] \in N$. Since $\langle x_0, x_1 \rangle \leq T^{\text{Id.}}$, we know that $[u, v] \in T^{\text{Id.}}$. Note now that $[g, h] \in T^{\text{Id.}} \cap (N \cap K)$.

Since N is normal in K or in T_{BB} Proposition 3.5.4 tells us that $N \cap K \trianglelefteq K$. Recall from Theorem 3.5.9 that $T^{\text{Id.}} \leq K$. We apply Proposition 3.5.4 and get that $T^{\text{Id.}} \cap (N \cap K) \trianglelefteq T^{\text{Id.}}$. But since T is simple, so is $T^{\text{Id.}}$. Since the intersection $T^{\text{Id.}} \cap (N \cap K)$ is non-trivial, it must be all of $T^{\text{Id.}}$. Thus $T^{\text{Id.}} \leq N$.

Since $T^{\delta\gamma^2}$ also has a copy of F which acts on the i strand, we can choose a non-trivial commutator that's in the intersection $T^{\delta\gamma^2} \cap (N \cap K)$. Then we apply the same argument and find that $T^{\delta\gamma^2} \leq N$.

The groups T^{γ} and $T^{\delta\gamma}$ have a copy of F that acts on the j strand. The j strand has red on the left and blue on the right. So if we change our initial color choice for S, we can find that both of these are in N. Similarly, choosing S to be between blue and green will give us that T^{γ^2} and T^{δ} are in N.

We have showed that $T^{\text{Id.}} \cup T^{\delta\gamma^2} \cup T^{\gamma} \cup T^{\delta\gamma} \cup T^{\gamma^2} \cup T^{\delta} \subseteq N$. These generate K. $\square$

Corollary 3.5.17. *The* $\ker \rho$ *is the double commutator subgroup* $\big[[T_{BB}, T_{BB}], [T_{BB}, T_{BB}]\big]$.

Proof. It is a fact that homomorphisms map commutator subgroups to commutator subgroups. So we know $\rho([T_{BB}, T_{BB}]) = [S_3, S_3] = A_3$. But also,

$$\rho\left(\left[[T_{BB}, T_{BB}], [T_{BB}, T_{BB}]\right]\right) = \left[[S_3, S_3], [S_3, S_3]\right] = [A_3, A_3] = \{e\}.$$

This implies that $\left[[T_{BB}, T_{BB}], [T_{BB}, T_{BB}]\right] \subseteq \ker \rho$. Since ρ is onto, we indeed have $\left[[T_{BB}, T_{BB}], [T_{BB}, T_{BB}]\right] = \ker \rho = K$. □

It is well know that if a subgroup H of G has finite index in G, then there exists a subgroup $N \leq H$ that is normal in G and also has finite index. This give us the following corollary.

Corollary 3.5.18. *The finite-index subgroups of T_{BB} all contain K and thus are in one-to-one correspondence with the subgroups of S_3.*

4
Other Julia Sets

We have spent some time exploring a few other Julia sets. We call the first one is for $\phi(z) = \frac{e^{2\pi i/3}z^2-1}{z^2-1}$. We call it the **Birds** Julia set. See Figure 4.0.1. (In all of our figures, the red points are part of an attracting cycle.)

Conjecture 4.0.19. *The group of homeomorphism from the Birds Julia set to itself is isomorphic a nonabelian groups of order eight.*

We are nearly certain this is true. However, we have the same difficulty in proving it as we did in the argument that associated triple point partners for the Bubble Bath. It really *looks* like there are only two triple points that will disconnect the Bird Set into two pieces. But again, proving this might require defining paths in the Julia set – which is hard. If we could do it, the proof begins by noticing that the two main four points are uniquely associated to each other. There are six other points which must be associated with each other. Then an induction on the main structures – the "birds" – shows that everything else must follow from the action on the first eight points.

The next Juliea set comes from the function $\phi(z) = \frac{z^2+1}{z^2-1}$. We call it the **Rigid Carpet** for its visual similarity to the Sierpinski Carpet, see Figure 4.0.2. We understand the Rigid

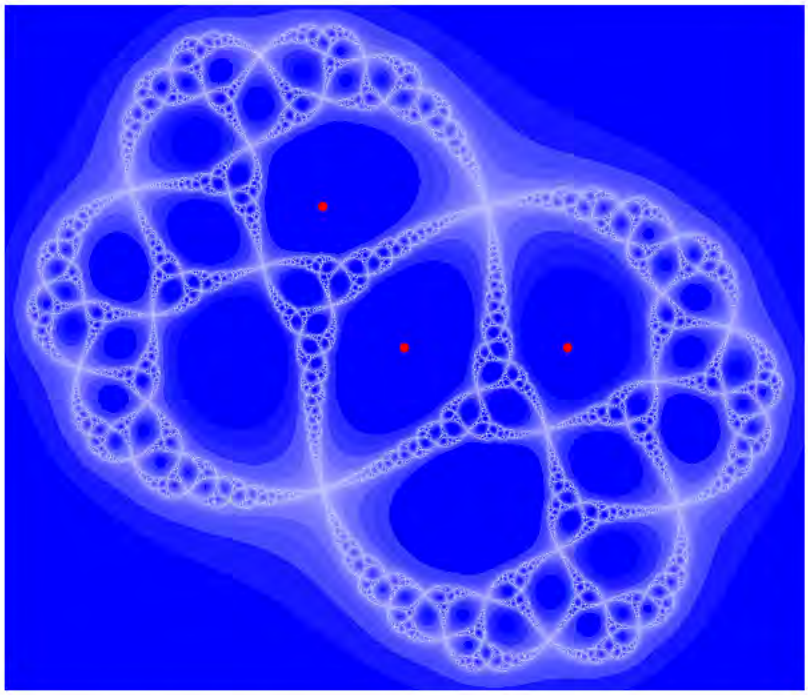

Figure 4.0.1: The function $\phi(z) = \frac{e^{2\pi i/3}z^2-1}{z^2-1}$ gives the Birds Julia set.

Carpet less thoroughly. But we believe that either the homeomorphism group is of finite order, or that it will be infinite but "rigid" in nature. In the first case, we expect the proof to be similar to that of the Birds Julia set. In the second case what we mean is that there are infinite homeomorphism but choosing a single point will define the entire homeomorphism – i.e. they are rigid and not "floppy" like our piecewise ones for the Bubble Bath.

Unfortunately, it appears that neither of these yield the Thompson-like groups we are interested.

The final Julia sets we have explored seem to be related to the Bubble Bath. See Figure 4.0.3. These functions have similar formulae to the Bubble Bath's function. They are given by $\phi(z) = c\frac{z^2-1}{z^2}$ for $c \approx 1.618$ and $c \approx 1.947$ respectively. It is almost trivial that these should have groups similar to T_{BB}. They look just like the Bubble Bath with some extra strands put in. All the methods we used should extend just fine for these.

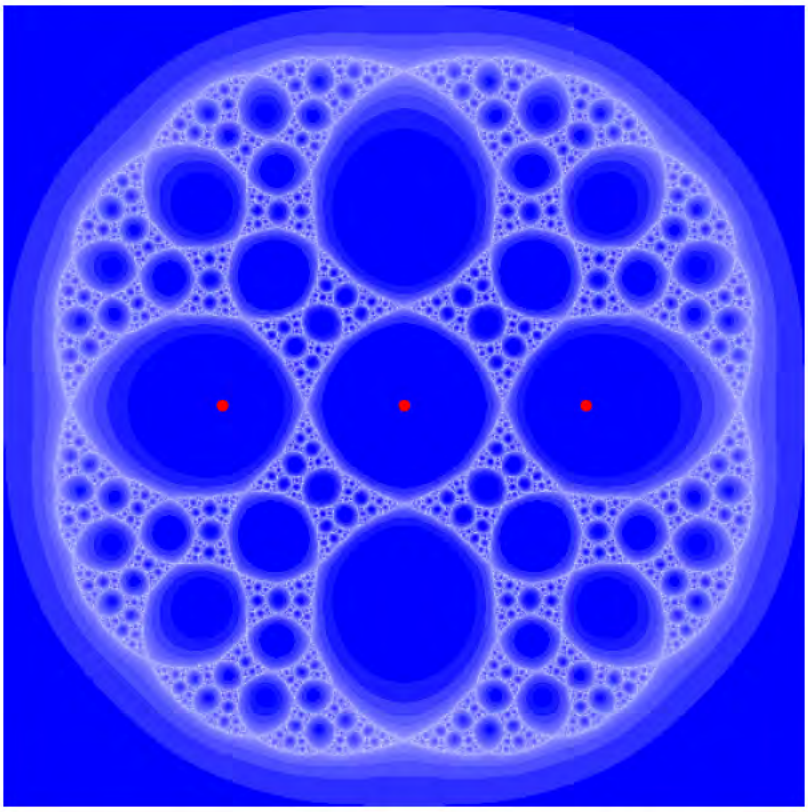

Figure 4.0.2: The function $\phi(z) = \frac{z^2+1}{z^2-1}$ gives the Rigid Carpet Julia set.

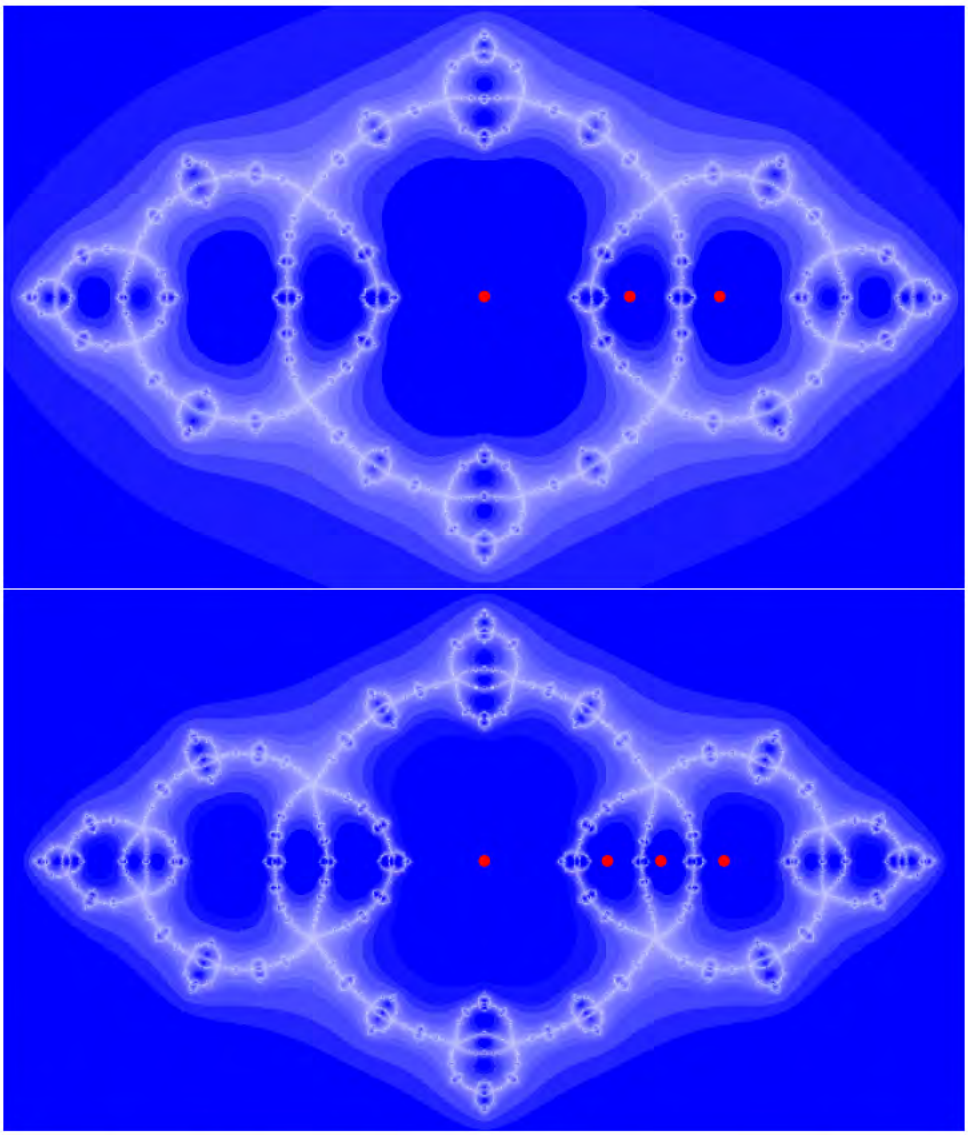

Figure 4.0.3: The function $\phi(z) = \frac{z^2+1}{z^2-1}$ gives the Rigid Carpet Julia set.

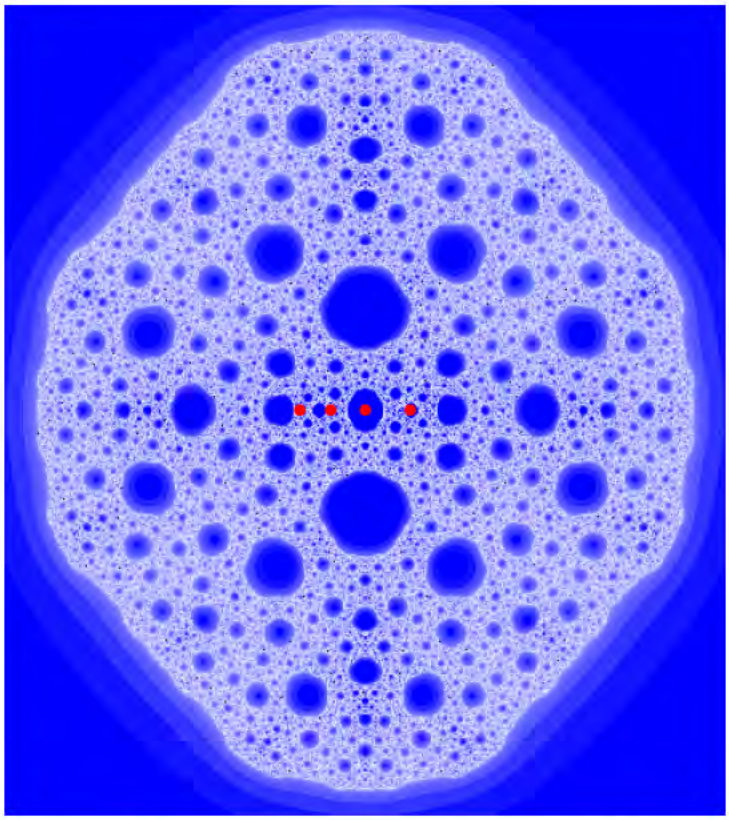

Figure 4.0.4: We are confused by the Egg Shell Julia set.

Besides these, there are a few other quadratic rational Julia sets with small attracting orbits. However, in the same way that there seems to be a whole class of Bubble Baths, there are other Birds Julia sets as well as other Rigid Carpets. There seems to be only one other class which appears in Figure 4.0.4. We could make head, nor tail, or bubbles out of these. They are quite confusing.

Future work could continue to investigate any of the Julia sets mentioned here. It could turn to cubic rational functions. Or it could try to approach the itinerary and geometric address techniques from a different angle and try to establish when they are applicable and when they are not. For instance, with more time, we would have liked to prove that as long as the function is hyperbolic, we can always implement these methods.

Bibliography

[1] Kathleen T. Alligood, Tim D. Sauer, and James A. Yorke, *Chaos an Introduction to Dynamical Systems*, Springer, New York, 1996.

[2] Luis Barreira, *Ergodic Theory, Hyperbolic Dynamics and Dimension Theory*, Springer, Berlin, 2012.

[3] James Belk, *Personal communication*, April 29th, 2013.

[4] James Belk and Bradley Forrest, *A Thompson Group for the Basilica*, Preprint (2012), arXiv:1201.4225v1 [math.GR].

[5] Matthew G. Brin, *The Ubiquity of Thompson's Group F in Groups of Piecewise Linear Homeomorphisms of the Unit Interval*, J. London Math. Soc. **60** (1999), no. 2, 449–460.

[6] Kenneth S. Brown, *Finiteness Properties of Groups*, Journal of Pure and Applied Algebra **44** (1987), 45-75.

[7] James Ward Brown and Ruel V Churchill, *Complex Variables and Applications*, McGraw-Hill, New York, 2009.

[8] Peter J. Cameron, *Permutation Groups*, Cambridge University Press, Cambridge, 1999.

[9] J.W. Cannon, W. J. Floyd, and W.R. Parry, *Introductory notes on Richard Thompson's groups*, Enseign. Math **42** (1996), 215–256.

[10] David S. Dummit and Richard M. Foote, *Abstract Algebra*, John Wiley and Sons, Hoboken, NJ, 2004.

[11] Graham. Higman, *Finitely presented infinite simple groups*, Notes on Pure Mathematics **8** (1974).

[12] John E. Hutchinson, *Fractals and Self Similarity*, Indiana University Mathematics Journal **30** (1981), no. 5, 713–747.

[13] John Milnor, *Dynamics in One Complex Variable*, Princeton University Press, Princeton, 2006.

[14] James R. Munkres, *Topology*, Pearson Prentice Hall, New Jersey, 2000.

[15] A.A. Puntambekar, *Formal Languages and Automata Theory*, Technical Publications, Pune, India, 2011.